FUDMA Journal of Earth and Environmental Sciences (FUDJEES), Vol. 3, No. 1, 2026
Print ISSN: 1595-9686
EISSN: 1595-9708

PRIORITIZATION OF SOIL EROSION RISK MANAGEMENT IN THE BUNSURU WATERSHED OF KATSINA STATE USING INTEGRATED MORPHOMETRIC ANALYSIS AND WEIGHTED SUM APPROACH

Aminu Kabir[1*] and Danjuma Jijuwa Ijafiya[2]
[1]Department of Geography, Federal University Lokoja, Nigeria
[2]Department of Geography, Federal University Dutsin-Ma, Katsina State

*Email address: aminu.kabir@fulokoja.edu.ng
https://doi.org/10/3303/jees.2026.0301/036

ABSTRACT
The Bunsuru watershed, one of the largest in Katsina State and the primary inflow source for the Zobe Reservoir, is vulnerable to erosion owing to its semi-arid climate and land use pressure. This underscores the need for a comprehensive strategy to prioritize erosion management within the watershed. Previous studies employed the compound factor method, which is inherently biased in weighting individual morphometric parameters. This study utilized SRTM-DEM data, Geographic Information Systems (GIS), and a novel weighted sum approach (WSA) to characterize and prioritize sub-watersheds. According to the WSA approach, the sub-watersheds were classified into very high, high, moderate, low, and very low erosion risk categories. The study found that 3 sub-watersheds covering 31.8% of the watershed area had a very high erosion risk, 20 sub-watersheds occupying 28.1% of the area had a high erosion risk, and 21 sub-watersheds covering 27.6% of the area had a moderate erosion risk. Meanwhile, 12.5% were low- and very low-erosion risk areas. The study recommends implementing urgent conservation measures, specifically afforestation and strict land-use enforcement, especially in the high-risk zones, to protect the downstream Zobe reservoir.

Keywords: Soil erosion, Morphometric analysis, Katsina State, Bunsuru Watershed.

INTRODUCTION

The Bunsuru Watershed serves as a vital hydrological lifeline for Katsina State; its role in sustaining the Zobe Reservoir is increasingly compromised by accelerated soil erosion driven by fragile semi-arid ecosystems and land-use pressures. (Adesoji et al., 2024). The semi-arid ecology is characterized by thin soils, sparse vegetation, and flashy rainfall, which increase vulnerability to soil erosion. The watershed's erosion susceptibility is compounded by anthropogenic activities such as farming, livestock rearing, deforestation, and construction. These activities initiate the removal and entrainment of topsoil, reducing soil fertility and productivity and exacerbating reservoir sedimentation and water quality degradation. (Arrington, 2021).

The consequences of erosion extend beyond the landscape, as high sediment yields are increasingly contributing to the siltation of Zobe reservoir. Reservoir sedimentation threatens not only the long-term viability of the Zobe reservoir for irrigation, but also causes habitat degradation for aquatic species (Adesoji et al., 2024). Furthermore, it increases water turbidity in the reservoir, with a growing impact on treatment costs for sustainable domestic water supply. Sustainable soil and water resource conservation underscores the need to prioritize soil erosion management. (Marcellus & Ehiomogue, 2017). However, there is a lack of systematic, data-driven prioritization to identify which sub-watersheds contribute most to the sediment load. Without a clear scientific ranking of these high-risk "hotspots," conservation efforts remain fragmented and inefficient, underscoring the need for soil erosion risk prioritization.

However, the conventional methodology for watershed prioritization is labour-intensive, time-consuming, and expensive. Thus, the advent of remote sensing and Geographic Information

System (GIS) capabilities has expedited and facilitated the characterization and prioritization of watersheds, rendering the process more efficient and cost-effective. Due to its high temporal resolution, remote sensing is an effective tool for monitoring landscape changes over time (Hegazy & Kaloop, 2015). Remote sensing also offers multi-spectral data, extensive ground coverage, and a digital image format. Thus, the use of remote sensing and GIS for watershed prioritization and morphometric characterization has evolved into a well-established methodology (Gajbhiye et al., 2014; Kandpal et al., 2017; Choudhari et al., 2018; Farhan et al., 2017; Kumar, 2021; Singh et al., 2021; Benzougagh et al., 2022; El-Brahimi et al., 2024).

A review of the existing literature shows that only a few scholars have recently researched watershed prioritization and characterization in Nigeria. Notable studies include Yonnana et.al (2020) on the Muvur watershed, Oruonye and Ahmed (2021), on the Lamurde River Basin, Odiji et al. (2021), on the upper Benue watershed, and Nwilo et al. (2021) on the Imo River Basin. However, except for the study conducted by Nwilo et al. (2021), the aforesaid studies focused on rivers in the northern region of the country. This exposed the paucity of studies in Northern Nigeria that integrated morphometric analysis with the Weighted Sum Approach (WSA) for watershed prioritization despite its advantages. Nevertheless, these studies utilized a compound factor prioritization method for sub-watersheds, relying on the basic arithmetic mean to determine priority rankings. This method is deficient because it uniformly assigns equal weight to all morphometric parameters without accounting for the watershed's unique characteristics, the relationship between the parameters and erosion, or the correlations among the morphometric parameters. Consequently, this approach may introduce bias in weighting individual morphometric parameters (Godif and Manjunatha, 2022).

Hence, Aher et al. (2014) proposed the utilization of the Weighted Sum Approach (WSA). The method entails an initial ranking of parameters, the creation of a correlation matrix, determining weights, estimating the compound factor, and subsequently prioritizing sub-watersheds. The advantage of the Weighted Sum Approach (WSA) lies in integrating correlation statistical analysis with ranking. The correlation analysis discerns the influence of each parameter on erosion, thereby eliminating parameters that may introduce bias into the final result (Sharma et al., 2015). Numerous authors have previously employed this approach for watershed prioritization (Malik et al., 2019; Godif & Manjunatha, 2022; Wagh & Manekar, 2023).

The Bunsuru Watershed, despite being one of the largest irrigation areas in Katsina State, has not yet been the subject of any research focused on soil erosion prioritization. This is needed to mitigate siltation and enhance the resilience of the downstream reservoir against floods. Furthermore, the economic sustenance of the residents in the watershed is entirely reliant on agriculture, underscoring the pivotal role of the watershed's condition in influencing the region's economy, particularly in the context of soil erosion. This circumstance emphasizes the need to prioritize soil erosion in the watershed. Such information is needed to pursue sustainable conservation practices. Hence, the study aimed to prioritize soil erosion risk management in the Bunsuru Watershed through an integrated method of morphometric analysis and a weighted Sum Approach. The objectives were to investigate the basic morphometric characteristics of the Bunsuru watershed, examine the morphometric attributes controlling soil erosion in the watershed, and prioritize the sub-watersheds based on their susceptibility to erosion.

MATERIALS AND METHODS

Description of the Study Area

The Bunsuru watershed is situated between 11º 56ˈ 30ˈ̎ N and 12º 16ˈ 0ˈ̎ North of the equator and between longitude 7º 31ˈ30ˈ̎ and 7º 44ˈ 30ˈ̎ East of the Greenwich meridian. The river flows in a northerly direction and occupies an area of 569.7 km^2 (Figure 1). The climate of the region is semi-arid, characterized by well-defined periods of wet and dry seasons. The rainy season occurs

FUDMA Journal of Earth and Environmental Sciences (FUDJEES), Vol. 3, No. 1, 2026
Print ISSN: 1595-9686
EISSN: 1595-9708

from May to October, with a maximum rainfall of 800mm. The rainfall is often flashy with high potential for surface encrustation, sediment removal and transport. Conversely, the dry season prevails from November to March. The vegetation in the region corresponds to the Sudan savannah, characterized by the prevalence of trees, shrubs, and grasses. However, a significant proportion of the trees have been removed, resulting in isolated patches forming scattered gallery forests. This altered landscape increases the vulnerability of the watershed to erosion. The study area is underlain by Precambrian Basement Complex rocks, whose prolonged weathering has produced predominantly ferruginous soils. These soils are generally characterized by low structural stability and high erodibility, rendering the area particularly susceptible to soil erosion. The hydrology of the basin exhibits a highly connected network that facilitates rapid runoff, enhances soil erosion, and increases sediment transport to the Zobe Reservoir, thereby reducing its operational lifespan (Obialor et al., 2019). The land use of the basin comprises mostly farming, grazing, and construction, which can increase the basin's vulnerability to erosion.

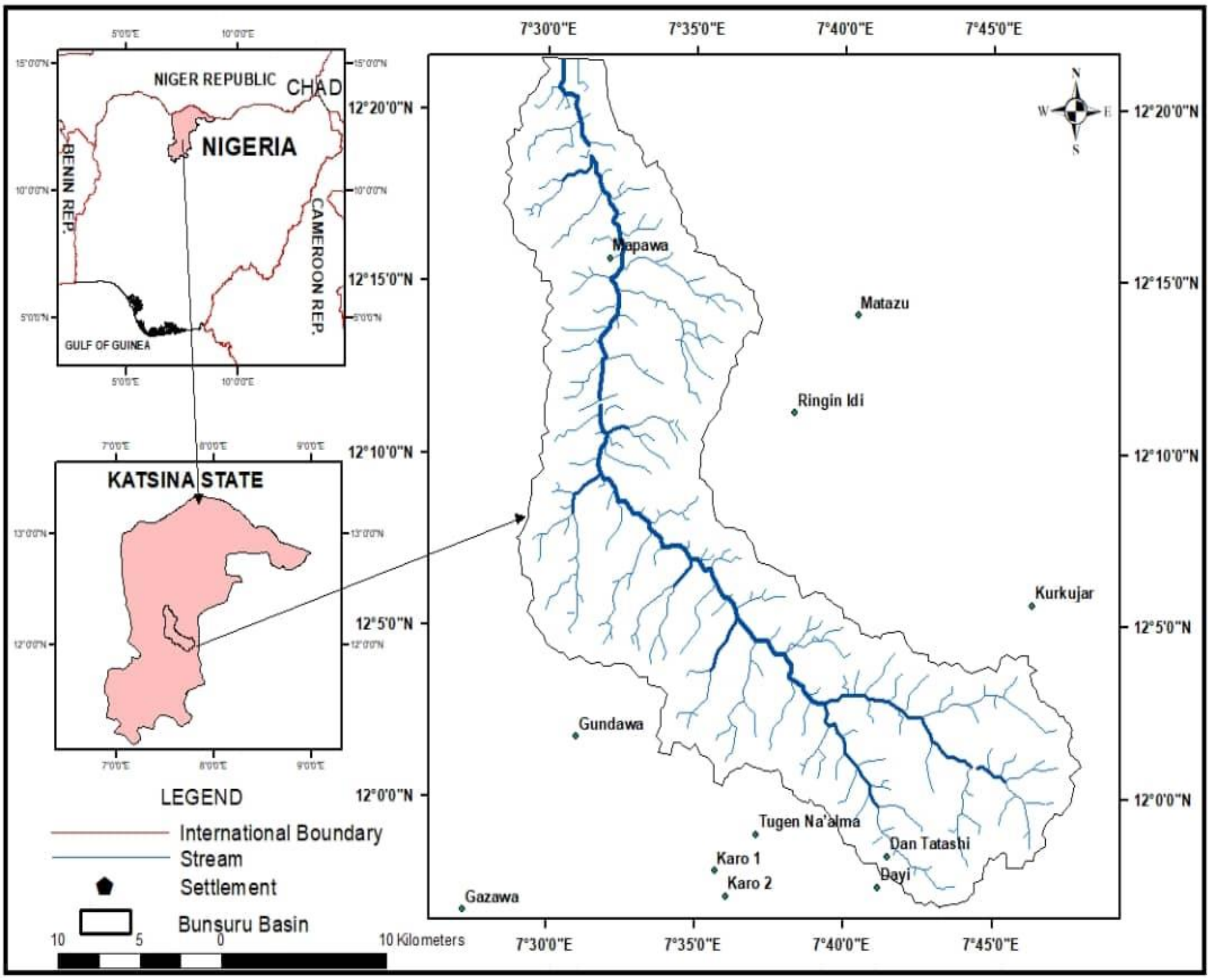

Figure 1: Study Area

Data Sources and Types

The Digital Elevation Model (DEM) simplifies, manages, and improves accuracy compared to the traditional method of manually extracting information (Forkuor & Maathuis, 2012). Thus, a 30-meter resolution DEM, derived from the Shuttle Radar Topographic Mission Plus (SRTM PLUS-DEM), was obtained from the United States Geological Survey's archive (https://earthexplorer.usgs.gov). The SRTM DEM offers the advantage of high-resolution data that is nearly global in coverage while maintaining homogeneity and consistency (Yang, 2011). However, it is prone to overestimating actual elevation, particularly in forested areas. (Shortridge, 2013). Thus, using only an automated DEM may limit accurate drainage network information (Turcotte et al., 2001). To improve precision, the topographic map of Dutsin-ma Southeast, at a scale of 1:50,000 and obtained from the Department of Survey in Katsina State, was scanned, geometrically corrected, digitized, and interpolated with ground survey data to recondition the DEM. Reconditioning the DEM using a high-resolution topographic map enhances its accuracy and Reliability (Callow et al., 2007). The data sources are presented in Table 1.

Table 1: Data sources and types

Type of Data	Resolution	Source of Data	Year	Purpose
SRTM- DEM	30 m	https://earthexplorer.usgs.gov	2015	Sub-watershed delineation and basic morphometric parameters extraction
Topographic map	1:50,000	Survey Department, Katsina State	1990	To recondition the SRTM DEM

Sub-watershed Delineation and Stream Network Extraction

The DEM and topographic map were mosaicked into a new raster dataset and projected to the WGS 1984, Zone 32º N spatial coordinate system. Sub-watersheds and stream networks were then generated using the spatial analysis tools in ArcGIS 10.8. These tools offer advantages over traditional manual tracing and extraction methods by automating the identification of surface water flow direction and the creation of stream networks (Maderal et al., 2016; Heine, et al., 2004). The DEM was reconditioned using the topographic map, which involved removing local depressions to ensure continuity of flow. Subsequently, fill, flow direction, flow accumulation, basin analysis, and stream ordering were performed with a threshold value of 0–100 for minor streams and 100 and above for major streams. This threshold was selected to enhance the appearance of streams and sub-watersheds. The linear attributes were determined, and errors in stream numbers and basin stream lengths were corrected through explode and planarize line analyses. In delineating the sub-watersheds, four points were generated and snapped to areas of higher flow accumulation, leading to the extraction of 59 sub-watersheds (Figure 2). These were then converted from raster to polygon format using the conversion tool. Consequently, the basin area, perimeter, basin length, maximum, minimum, average elevation, stream order, and stream length were analyzed for each sub-watershed.

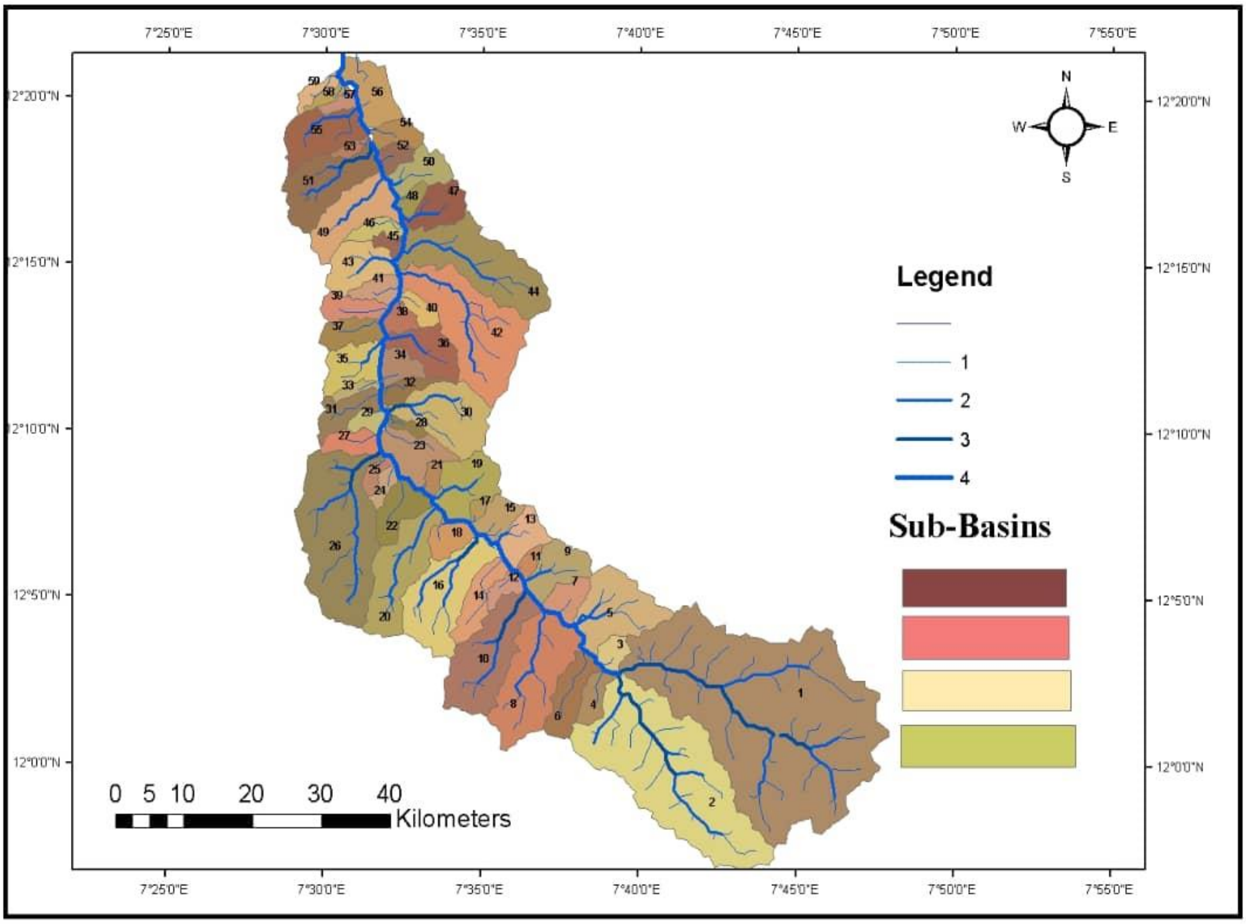

Figure 2: The Sub-watersheds

Measurement of morphometric parameters

Following the sub-watershed delineation and the drainage network generation, fundamental morphometric parameters for each sub-watershed, such as area, perimeter, basin length, stream order, stream number, stream length, maximum and minimum elevation, and mean height, were extracted using ArcGIS 10.8 processing tools. The other parameters related to soil erosion were calculated using the standard mathematical equations provided in Table 2. These include linear, areal, and topographic parameters.

Table 2: Morphometric variables sensitive to soil erosion

S/No.	Aspect	Morphometric Variables	Formula/Description	References
1	Basic	Basin area *(A)*	Watershed boundary (Km^2)	(Schumm, 1956)
2		Basin perimeter *(p)*	Perimeter of a watershed (km)	(Schumm, 1956)
3		Basin length *(L_b)*	The basin's longest distance parallel to the drainage line (km)	(Schumm, 1956)
4		Maximum Elevation *($M_{ax\ e}$)*	Elevation of the lowest cell in the Watershed (m)	DEM
5		Minimum Elevation *($M_{in\ e}$)*	Elevation of the highest cell in the Watershed (m)	DEM
6		Mean Height *($M_{ean\ e}$)*	Mean Height of all cells in the Watershed (m)	DEM
7		Stream order *(N)*	Streams hierarchical order	(Strahler, 1957)
8		Stream length	Total length of a stream of a particular order (km)	(Strahler, 1964)
9		Streams Number	Total number of streams of all orders	(Horton, 1945)
10	Linear	Drainage density	Drainage Density (D_d) = $\frac{Lu}{A}$	(Strahler, 1956)
11		Stream frequency	F_s $\frac{Number\ of\ streams}{Area}$	(Strahler, 1964)
12		Texture ratio *(R_t)*	$R_t = Ns/P$ (km^{-1})	(Horton, 1945)
13		Length of overland flow *(Lof)*	$L_of = (2 \times D_d)$ presented in (km)	(Horton, 1945)
14		A constant of channel maintenance *(C_{cm})*	$C_{cm} = (\frac{1}{Dd})$ (km)	(Strahler, 1964)
15	Areal	Form factor *(F_f)*	$F_f = \frac{A}{Lb^2}$	(Strahler, 1956)
16		Elongation ratio *(R_e)*	$Re = \sqrt{(Au)/\pi} / Lb$ Where A is the area of the basin, $\pi = 3.14$, and Lb is the basin length.	(Schumm, 1956)
17		Circularity ratio *(R_c)*	$R_c = \frac{4\pi A}{P^2}$	(Schumm, 1956)
18		Compactness coefficient	$\frac{P}{0.282 \times \sqrt{A}}$	(Horton, 1945)
19	Topographic	Basin relief	$R = (H_{max} - H_{min})$ (m). H_{max} refers to the maximum height (m). H_{min} is the minimum height (m).	(Strahler, 1964)
20		Ruggedness Number	$R_N = \frac{D_d}{R/1000}$	(Strahler, 1956)
21		Relative Relief *(R_{vr})*	$Rv_r = \frac{R}{P}$	(Schumm, 1956)
22		Relief Ratio	$R_r = \frac{R}{L_b}$	(Schumm, 1956)

Sub-watershed prioritization using the weighted sum approach

Sub-watershed prioritization is essential due to the varying responses of different sub-watersheds to soil erosion, highlighting the need for targeted conservation and management efforts. The weighted sum approach (WSA) was employed for this prioritization. The WSA methodology involves several key steps, including preliminary parameter ranking, correlation matrix generation, weightage computation, compound factor estimation, and final ranking. (Godif & Manjunatha, 2022). The preliminary ranking of sub-watersheds was done based on estimated values of morphometric parameters that are sensitive to soil erosion. Previous studies have shown that areal parameters exhibit a negative correlation with soil erosion, whilst linear and topographic parameters are positively correlated with soil erosion. (Thakkar & Dhiman, 2007). For parameters positively related to erosion, such as linear and relief parameters, a rank of 1 was assigned to the highest value, followed by a rank of 2 for the second-highest value, and so forth. Conversely, for morphometric attributes inversely related to erosion, such as areal, a rank of 1 was given to the smallest value, with a rank of 2 assigned to the next higher value (Malik et al., 2019). However, sub-watersheds with equal parameter values were assigned the same rank (Aher et al., 2014).

A correlation matrix was generated to examine the relationships among soil erosion-sensitive morphometric attributes. This matrix was utilized to calculate the weight of each morphometric parameter on soil erosion. The weight for each parameter was determined by dividing the sum of its correlation coefficients by the total. The correlation coefficients for each parameter were aggregated by summing the values across the corresponding rows of the correlation matrix. Subsequently, the total was obtained by summing all the elements within the matrix columns. The compound factor (CF) for each parameter was then calculated by dividing the sum of the respective correlated values by the total. These CF values were subsequently employed to rank the sub-watersheds, following the methodology outlined by Aher et al. (2014).

$$\sum_{j=1}^{N} \sum_{j=1}^{M} (W_j \times R_i) \tag{1}$$

In this context, W_j represents the weight of the parameter generated from the correlation matrix, while denotes the rank assigned to the ith parameter during the preliminary ranking. Additionally, N indicates the total number of parameters, and M represents the total number of ranks. The compound factor was subsequently multiplied by the preliminary priority ranking of each parameter to obtain the weight of each parameter for the overall priority ranking of the sub-watersheds as presented in the following equation.

$$\text{Prioritization} \quad (CF \times ppr\ of\ Dd) + (CF \times ppr\ of\ Fs) + (CF \times ppr\ of\ Rt) + (CF \times ppr\ of\ Lof) + (CF \times ppr\ of\ Ccm) + (CF \times ppr\ of\ Ff) + (CF \times ppr\ of\ Re) + (CF \times ppr\ of\ Cc) + (CF \times ppr\ of\ Rc) + (CF \times ppr\ of\ R) + CF \times ppr\ of\ RN) + (CF \times ppr\ of\ Rr) + (CF \times ppr\ of\ Rvr) \tag{2}$$

The sub-watersheds were categorized into very-high, high, medium, low, and very-low erosion risk zones based on the weight of each parameter corresponding to the ranges of less than 13.9, 14-16.9, 17-19.9, 20-21.9, and greater than 22, respectively, as per the scaling pattern adopted by many scholars (Aher et al., 2014; Choudhari et al., 2018; Godif & Manjunatha, 2022; Wagh, 2022; Dofee et al., 2024; Duressa et al., 2024).

RESULTS AND DISCUSSION

ANALYSIS OF THE BUNSURU WATERSHED MORPHOMETRIC PARAMETERS

Basic parameters of the Bunsuru Watershed

These parameters are crucial for characterizing the watershed, as they define its area, shape, and other physical attributes. The Bunsuru watershed covers an area of 569.7 km² with a total perimeter of 792.543 km (Table 3). The areas of the Bunsuru sub-watersheds range from 1.2 km² in SW 53 to 110 km² in SW 1, as shown in Figure 3. Sub-watersheds with larger areas exhibit high rates of soil erosion, consistent with the findings of Farhan et al. (2017) in the Zerqa watershed of Jordan. This occurs because larger surface areas of the sub-watersheds increase the volumes of rainfall, which can disintegrate soil particles. The perimeters of the sub-watersheds vary from 4.1 km in SW 17 to 54.9 km in SW 1. Although larger perimeters typically correlate with higher soil erosion, this is not uniform across all Bunsuru sub-watersheds. For example, despite SW 17 having the smallest perimeter, it demonstrates a high susceptibility to erosion, aligning with the findings of Duressa. et al. (2024) in the Darbus watershed of Ethiopia. This underscores the importance of considering the influence of land use, climate, vegetation, and other contributing factors when ranking sub-watersheds, as these elements can significantly affect erosion vulnerability, leading to variations that may not be solely attributed to physical characteristics. (Shekar et al., 2023).

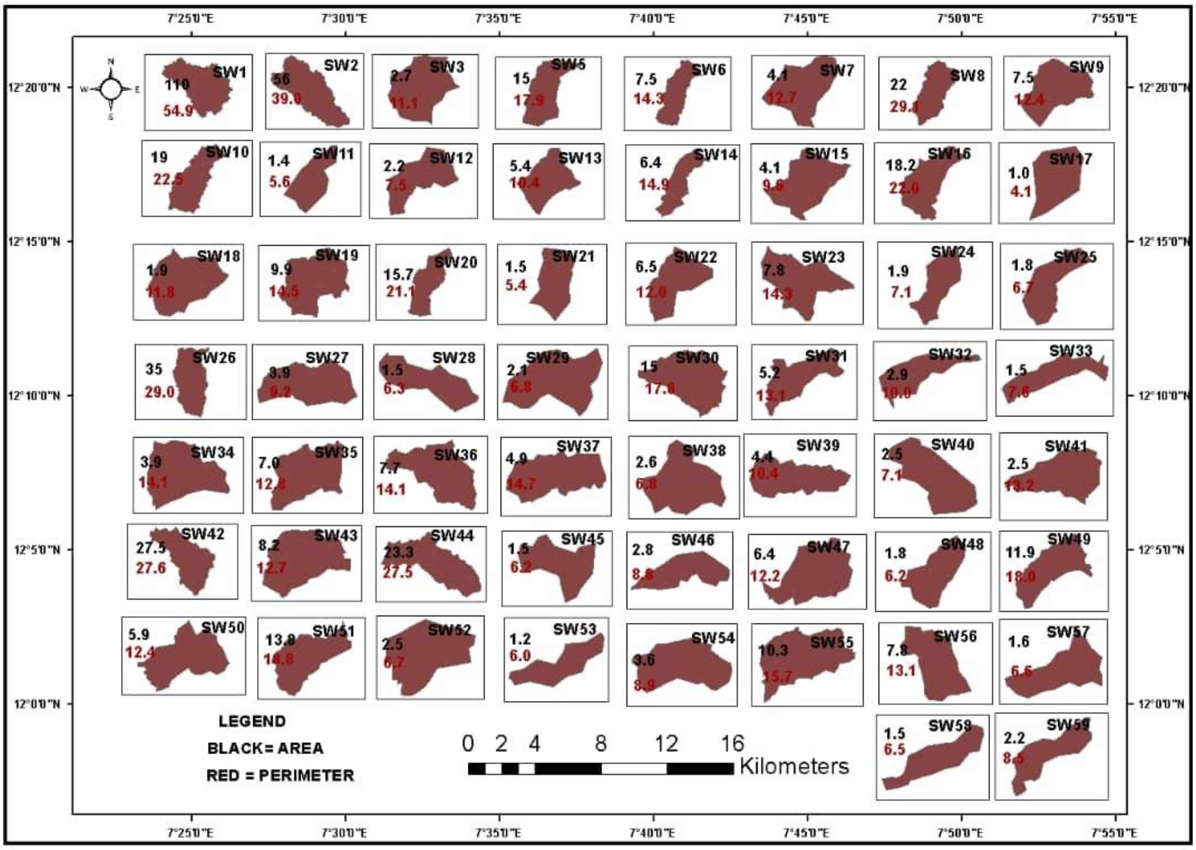

Figure 3: Perimeter and area of the Bunsuru sub-watersheds.

Table 3: Basic Morphometric Parameters of the Study Area

Sub-Watershed	Area (Km^2)	Perimeter (Km)	Basin Length (Km)	Max Elev (H_{max})	Min Elev (H_{min})	Mean Height (H_{mean})
SW1	110	54.9	16.1	646	575	611.58
SW2	56	39.0	13.6	648	574	606.66
SW3	2.7	11.5	2.2	595	572	582.66
SW4	3.8	10.0	3.1	603	573	585.15
SW5	15	17.9	5.7	609	557	582.68
SW6	7.5	14.3	5.1	608	561	586.80
SW7	4.1	12.7	2.6	588	554	571.79
SW8	22	29.1	8.1	613	552	583.12
SW9	7.5	12.4	4.1	587	548	572.04
SW10	19	22.5	8.1	609	548	583.69
SW11	1.4	5.6	2.2	578	547	564.18
SW12	2.2	7.5	2.6	578	547	563.97
SW13	5.4	10.4	3.2	584	545	564.60
SW14	6.4	14.9	5.6	594	544	572.86
SW15	4.1	9.6	2.9	580	540	560.80
SW16	18.2	22.0	7.2	602	540	575.19
SW17	1.0	4.1	1.6	572	539	559.13
SW18	1.9	11.8	2.1	577	540	557.43
SW19	9.9	14.5	4.6	580	531	559.27
SW20	15.7	21.1	7.8	605	535	571.68
SW21	1.5	5.4	1.8	563	531	549.29
SW22	6.5	12.0	4.1	575	526	552.08
SW23	7.8	14.3	4.3	570	522	543.83
SW24	1.9	7.1	2.8	564	524	542.26
SW25	1.8	6.7	2.5	556	526	541.84
SW26	35	29.0	9.7	602	525	567.97
SW27	3.9	9.2	3.5	567	524	544.75
SW28	1.5	6.3	2.6	549	519	536.24
SW29	2.1	6.8	2.5	553	518	535.87
SW30	15	17.8	5.9	579	519	551.73
SW31	5.2	13.1	4.5	566	518	543.21
SW32	2.9	10.0	3.7	553	517	532.25
SW33	1.5	7.6	2.8	552	516	536.78
SW34	3.9	14.1	2.6	550	517	533.59
SW35	7.0	12.8	4.5	554	512	535.26
SW36	7.7	14.1	5.0	601	509	540.90
SW37	4.9	14.7	3.7	547	510	533.71
SW38	2.6	6.8	2.0	586	507	521.94
SW39	4.4	10.4	4.0	547	510	533.71
SW40	2.5	7.1	2.8	572	508	530.80
SW41	2.5	13.2	3.3	540	507	521.08
SW42	27.5	27.6	9.2	575	506	542.16
SW43	8.2	12.7	4.1	548	505	528.11
SW44	23.3	27.5	9.0	565	502	532.20
SW45	1.5	6.2	1.9	528	501	541.20
SW46	2.8	8.8	3.5	539	503	519.96
SW47	6.4	12.2	4.0	536	502	521.59
SW48	1.8	6.2	1.8	523	500	511.42
SW49	11.9	18.0	6.3	547	498	520.83
SW50	5.9	12.4	3.4	533	499	516.87
SW51	13.8	18.8	6.6	541	496	520.38
SW52	2.5	6.7	2.2	523	498	510.12
SW53	1.2	6.0	2.3	520	497	506.52
SW54	3.6	8.9	3.3	530	496	514.21
SW55	10.3	15.7	5.4	533	495	511.96
SW56	7.8	13.1	2.5	525	493	502.23
SW57	1.6	6.6	1.4	514	494	499.38
SW58	1.5	6.5	2.9	520	493	506.50
SW 59	2.2	8.5	3.4	523	493	507.70

The Basin lengths range from 1.4 km in sub-basin 53 to 16.1 km in sub-basin 1. Sub-watersheds 1, 2, 5, 6, 8, 10, 16, 20, 26, 36, 44, 49, 51, and 55 have relatively greater lengths, each exceeding 5 km, while others have shorter lengths, measuring less than 5 km. Sub-watersheds with longer lengths exhibit high susceptibility to erosion, as greater length increases the volume and velocity of runoff, dislodging and transporting soil particles, as similarly observed by Bagarello et al. (2010). The maximum elevation in the basin measures 648 m in SW 2, while the minimum elevation is observed to be 493 m in SW 56. Sub-watersheds with maximum heights exhibit greater vulnerability to erosion, while those with lower elevations show less susceptibility. This observation aligns with the general principle that higher relief is associated with steeper slopes, which increases the potential for erosion (Raja Shekar & Mathew, 2024).

Stream order is another important parameter for characterizing watersheds and assessing their susceptibility to erosion. Additionally, related parameters such as stream number and length, directly influenced by stream order, are valuable for watershed characterization and can be effectively utilized in prioritization. Stream order is the classification of a stream's position within the hierarchical network of the drainage system (Obeidat et al., 2021). In hydrological terms, a fingertip stream is a first-order stream. When two first-order streams converge, they form a second-order stream, and the junction of two second-order streams forms a third-order stream, and so forth. It is noted that within the study area, eight sub-watersheds (SW 1, 2, 5, 10, 16, 26, 30, and 51) are of third-order, fourteen sub-watersheds (SW 8, 9, 19, 20, 33, 34, 40, 41, 42, 45, 47, 48, 49, and 51) are of second-order, and thirty-seven sub-watersheds (SW 3, 4, 6, 7, 11, 12, 13, 14, 15, 17, 18, 21, 22, 23, 24, 25, 27, 28, 31, 32, 35, 36, 37, 38, 39, 43, 44, 46, 50, 51, 52, 54, 55, 56, 57, 58, and 59) are of first-order.

Analysis of stream number shows that the streams decrease as stream order increases, since higher-order streams form from the junction of two or more lower-order streams. This pattern aligns with Horton's (1945) law of stream number. Also, the relationship between stream order, stream number, and stream length in each of the Bunsuru sub-watersheds is presented in Table 4. The results show that the sub-watersheds comprise 152 first-order streams (78%), 34 second-order streams (17.4%), and 9 third-order streams (4.6%), resulting in a total of 195 streams within the entire watershed (Figure 4). Sub-watershed 1 has the highest number of streams, with 33, whereas sub-watersheds 3, 4, 6, 7, 11, 12, 14, 17, 18, 21, 22, 23, 24, 25, 27, 28, 29, 31, 32, 37, 38, 39, 46, 52, 54, 58, and 59 each contain only 1 stream. Furthermore, sub-watershed 1 exhibits the longest total stream length at 68.9 km, whereas sub-watersheds 11, 21, and 48 have the shortest total stream length, each measuring 0.4 km (Figure 5). The results also show that stream length decreases as stream order increases, with first-order streams having the longest stream length and third-order streams the shortest. These findings are consistent with those reported by Abdeta et al. (2020).

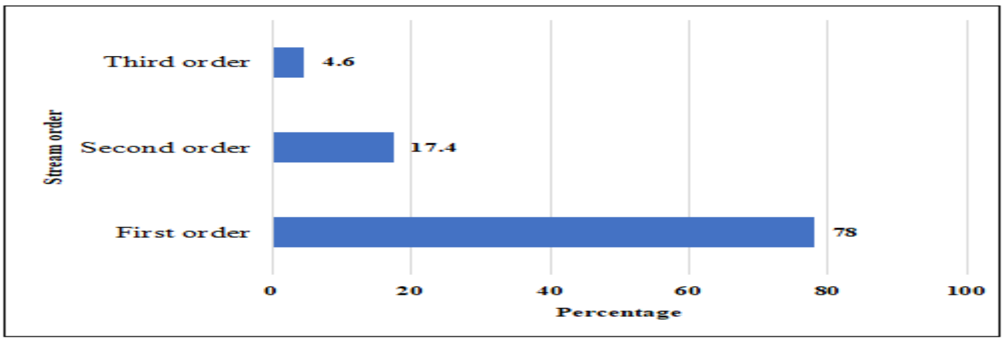

Figure 4: Stream ordering system in the Bunsuru watershed

FUDMA Journal of Earth and Environmental Sciences (FUDJEES), Vol. 3, No. 1, 2026
Print ISSN: 1595-9686
EISSN: 1595-9708

Table 4: Stream order, stream number, and stream length of each sub-watershed

Sub-watershed	I		II		III		Total	
	Sn	Sl	Sn	Sl	Sn	Sl	Sn	Sl
SW 1	27	41.6	4	14.3	2	13.0	33	68.9
SW 2	12	20.1	4	10.0	1	7.2	17	37.3
SW 3	1	0.9	0	0.0	0	0.0	1	0.9
SW 4	1	2.2	0	0.0	0	0.0	1	2.2
SW 5	4	7.2	2	3.7	1	0.1	7	11
SW 6	1	4.3	0	0.0	0	0.0	1	4.3
SW 7	1	1.0	0	0.0	0	0.0	1	1
SW 8	4	7.1	1	5.4	0	0.0	5	12.5
SW 9	3	3.1	1	1.7	0	0.0	4	4.8
SW 10	4	3.2	2	3.5	1	3.3	7	10
SW 11	1	0.4	0	0.0	0	0.0	1	0.4
SW 12	1	1.4	0	0.0	0	0.0	1	1.4
SW 13	2	2.2	0	0.0	0	0.0	2	2.2
SW 14	1	4.9	0	0.0	0	0.0	1	4.9
SW 15	2	1.8	0	0.0	0	0.0	2	1.8
SW 16	4	4.9	2	6.6	1	1.9	7	13.4
SW 17	1	0.6	0	0.0	0	0.0	1	0.6
SW 18	1	1.3	0	0.0	0	0.0	1	1.3
SW 19	3	1.7	1	2.9	0	0.0	4	4.6
SW 20	5	3.2	1	6.7	0	0.0	6	9.9
SW 21	1	0.4	0	0.0	0	0.0	1	0.4
SW 22	1	2.9	0	0.0	0	0.0	1	2.9
SW 23	1	3.7	0	0.0	0	0.0	1	3.7
SW 24	1	1.3	0	0.0	0	0.0	1	1.3
SW 25	1	0.7	0	0.0	0	0.0	1	0.7
SW 26	11	9.9	3	9.8	1	3.0	15	22.7
SW 27	1	1.8	0	0.0	0	0.0	1	1.8
SW 28	1	1.5	0	0.0	0	0.0	1	1.5
SW 29	1	0.5	0	0.0	0	0.0	1	0.5
SW 30	4	6.5	2	4.0	1	1.4	7	11.9
SW 31	1	3.3	0	0.0	0	0.0	1	3.3
SW 32	1	1.5	0	0.0	0	0.0	1	1.5
SW 33	1	1.4	1	0.0	0	0.0	2	1.4
SW 34	1	1.1	1	0.0	0	0.0	2	1.1
SW 35	2	2.5	0	1.8	0	0.0	2	4.3
SW 36	2	1.7	0	2.9	0	0.0	2	4.6
SW 37	1	2.6	0	0.0	0	0.0	1	2.6
SW 38	1	0.6	0	0.0	0	0.0	1	0.6
SW 39	1	2.9	0	0.0	0	0.0	1	2.9
SW 40	1	1.4	1	0.0	0	0.0	2	1.4
SW 41	1	1.9	1	0.0	0	0.0	2	1.9
SW 42	5	9.8	1	8.8	0	0.0	6	18.6
SW 43	3	2.1	0	2.4	0	0.0	3	4.5
SW 44	5	6.9	0	6.4	0	0.0	5	13.3
SW 45	1	0.5	1	0.0	0	0.0	2	0.5
SW 46	1	2.3	0	0.0	0	0.0	1	2.3
SW 47	2	1.8	1	2.3	0	0.0	3	4.1
SW 48	1	0.4	1	0.0	0	0.0	2	0.4
SW 49	2	1.3	2	3.9	0	2.7	4	7.9
SW 50	2	2.8	0	0.8	0	0.0	2	3.6
SW 51	4	2.5	0	3.4	1	0.0	5	5.9
SW 52	1	0.9	0	0.0	0	0.0	1	0.9
SW 53	1	0.8	1	0.0	0	0.0	2	0.8
SW 54	1	1.8	0	0.0	0	0.0	1	1.8
SW 55	2	2.9	0	3.7	0	0.0	2	6.6
SW 56	2	3.1	0	0.0	0	0.0	2	3.1
SW 57	2	1.9	0	0.0	0	0.0	2	1.9
SW 58	1	9.4	0	0.0	0	0.0	1	9.4
SW 59	1	2.2	0	0.0	0	0.0	1	2.2
Total	152	216.6	34	105	9	32.6	195	354.2
Percentage	78	61.2	17.4	29.6	4.6	9.2	100	100

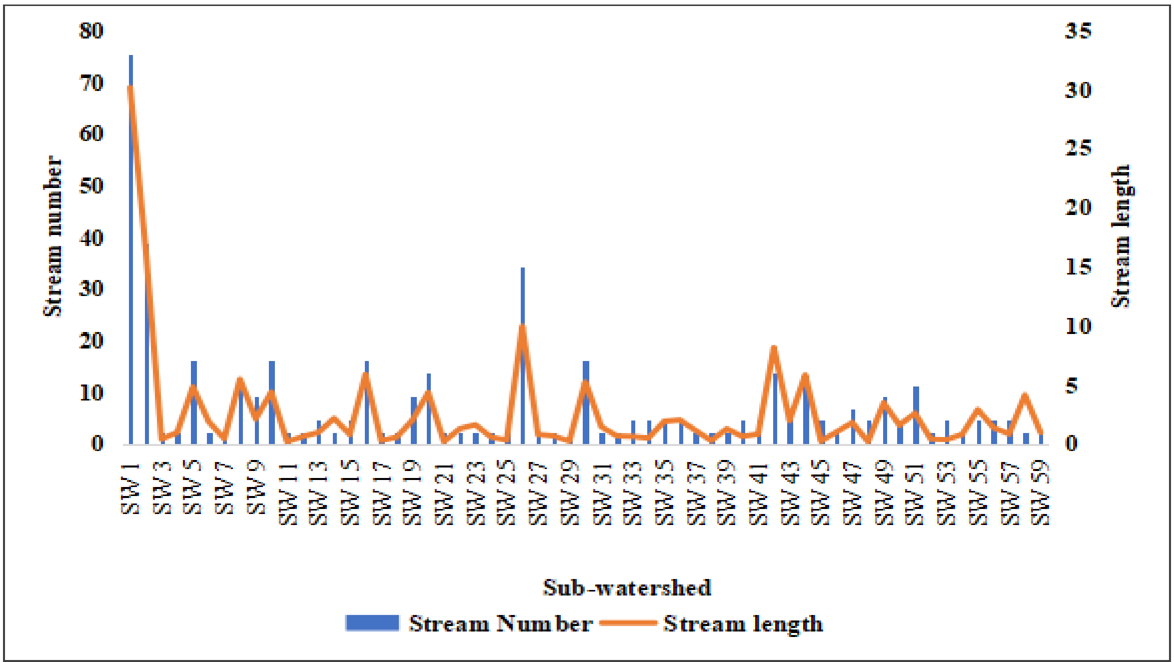

Figure 5: Stream number and length in the Bunsuru watershed

Areal characteristics of the Bunsuru Watershed

The areal parameters characterize the major stream and its tributaries, from the drainage divide to the basin's mouth, under structural and lithological controls within the watershed (Figure 6). These features include drainage density, stream frequency, elongation ratio, length of overland flow, and the constant of channel maintenance, which were used to assess the erosion susceptibility of the sub-watersheds. The computed values of these parameters are presented in Table 5. Drainage density values range from 0.22 km^2 in SW 48 to 1.19 km^2 in SW 57. Sub-watersheds with lower drainage density values indicate permeable surface material, higher infiltration rates, lower runoff, and reduced erosion potential. In contrast, sub-watersheds with relatively higher drainage density reflect less permeable geology, increased runoff, and higher erosion potential (Dragičević et al., 2019). Stream frequency was low, ranging from 0.13 in SW 56 to 1.00 in SW 17. A low stream frequency indicates fewer streams, lower hydrological activity, and minimal erosion potential (Raja Shekar & Mathew, 2024). All the sub-watersheds in the study area exhibit coarse drainage textures, with SW 37 and SW1 having the lowest and highest values, respectively. This variation reflects differences in the spacing of drainage lines, where areas of permeable geology have fewer drainage lines, whilst impermeable regions exhibit a higher density of drainage lines, as noted by Aher et al. (2014).

The length of overland flow in the sub-watersheds is relatively high, ranging from 0.06 km in SW 37 to 0.60 km in SW 1. This indicates that rainfall travels considerable distances before reaching the stream channels, which is consistent with the basin's gentle slope. Basins with gentle slopes typically have longer flow paths (Altaf et al., 2013). The findings also reinforce the assertion of low hydrological activities in the basin. The constant of channel maintenance varies from 0.84 in SW 57 to 4.55 in SW 48. A lower value, such as 0.84, signifies that 0.84 square feet is required to create one linear foot of the stream channel, while a higher value of 4.55 suggests that 4.55 square feet are needed. These results corroborate the findings of Hassan and Kabir (2019) in the Gada River Basin, Nigeria. Sub-watersheds with lower C values reflect sub-surface impermeability and low infiltration capacity, and vice versa, as reported by Dar et al. (2013).

FUDMA Journal of Earth and Environmental Sciences (FUDJEES), Vol. 3, No. 1, 2026
Print ISSN: 1595-9686
EISSN: 1595-9708

Table 5: Morphometric parameters of the Bunsuru watershed

Sub-Watershed	Areal			Linear						Topographic			
	D_d	F_s	R_t	L_{of}	C_{cm}	F_f	R_e	C_c	R_c	R	R_N	R_r	R_{vr}
SW1	0.63	0.30	0.60	1.26	1.58	0.02	0.71	1.48	0.46	71	0.04	1.03	1.18
SW2	0.67	0.27	0.38	1.34	1.49	0.04	0.68	1.56	0.46	74	0.05	1.98	1.66
SW3	0.33	0.37	0.08	0.06	3.03	0.33	0.97	1.97	0.26	23	0.01	0.03	5.17
SW4	0.58	0.26	0.10	1.16	1.72	0.79	0.74	1.45	0.48	30	0.02	0.01	6.03
SW5	0.73	0.47	0.05	1.46	1.36	0.12	0.66	1.30	0.59	52	0.04	0.00	3.40
SW6	0.60	0.13	0.07	1.20	1.66	0.37	0.73	1.47	0.46	47	0.03	0.01	4.25
SW7	0.24	0.24	0.08	0.48	4.16	0.43	1.14	1.77	0.32	34	0.01	0.03	4.63
SW8	0.56	0.23	0.17	1.12	1.78	0.14	0.74	1.75	0.33	61	0.03	0.00	2.11
SW9	0.64	0.53	0.32	1.28	1.56	0.33	0.70	1.28	0.61	39	0.02	0.01	4.73
SW10	0.53	0.37	0.31	1.06	1.89	0.19	0.77	1.46	0.47	61	0.03	0.01	2.71
SW11	0.29	0.71	0.18	0.58	3.45	0.87	1.05	1.34	0.56	31	0.01	0.08	10.32
SW12	0.64	0.46	0.45	1.28	1.56	1.12	0.71	1.43	0.49	31	0.02	0.02	7.71
SW13	0.41	0.37	0.19	0.82	2.44	1.12	0.88	1.21	0.63	39	0.02	0.02	5.27
SW14	0.76	0.16	0.18	1.52	1.32	0.27	0.65	1.66	0.36	50	0.04	0.01	3.99
SW15	0.43	0.49	0.21	0.86	2.33	1.27	0.85	1.33	0.56	40	0.02	0.02	6.04
SW16	0.74	0.38	0.32	1.48	1.35	0.19	0.66	1.46	0.47	62	0.04	0.01	2.74
SW17	0.60	1.00	0.24	1.20	1.67	0.27	0.73	1.16	0.75	33	0.02	0.10	13.95
SW18	0.68	0.53	0.08	1.36	1.47	1.12	0.36	2.42	0.17	37	0.03	0.03	4.88
SW19	0.46	0.40	0.28	0.92	2.17	0.47	0.82	1.30	0.59	49	0.02	0.01	4.00
SW20	0.63	0.38	0.28	1.26	1.59	0.16	0.71	1.50	0.44	70	0.04	0.01	2.86
SW21	0.26	0.67	0.19	0.52	3.85	0.93	1.09	1.24	0.65	32	0.01	0.08	10.43
SW22	0.45	0.20	0.08	0.90	2.22	0.77	0.84	1.33	0.57	49	0.02	0.02	4.79
SW23	0.47	0.15	0.07	0.94	2.13	0.57	0.82	1.44	0.48	48	0.02	0.01	3.98
SW24	0.68	0.53	0.14	1.36	1.47	1.12	0.68	1.45	0.47	40	0.03	0.03	7.94
SW25	0.38	0.56	0.14	0.76	2.63	0.36	0.90	1.41	0.50	30	0.01	0.04	8.29
SW26	0.65	0.43	0.52	1.30	1.54	0.06	0.70	1.38	0.52	77	0.05	0.00	2.07
SW27	0.46	0.26	0.11	0.92	2.17	1.20	0.82	1.31	0.58	43	0.02	0.02	6.16
SW28	0.71	0.67	0.16	1.42	1.41	0.67	0.57	1.45	0.47	30	0.02	0.02	8.71
SW29	0.23	0.48	0.15	0.46	4.34	0.84	1.16	1.32	0.57	35	0.01	0.07	8.13
SW30	0.79	0.47	0.39	1.58	1.27	0.11	0.63	1.29	0.59	60	0.05	0.01	3.25
SW31	0.63	0.19	0.08	1.26	1.59	0.48	0.71	1.62	0.38	48	0.03	0.01	4.32
SW32	0.51	0.34	0.10	1.02	1.96	1.29	0.78	1.66	0.36	36	0.02	0.02	5.53
SW33	0.93	0.67	0.01	1.86	1.08	0.77	0.58	1.75	0.33	36	0.03	0.03	7.26
SW34	0.28	0.26	0.07	0.56	3.57	0.32	1.06	2.01	0.25	33	0.01	0.03	3.90
SW35	0.61	0.43	0.23	1.22	1.64	0.38	0.72	1.36	0.54	42	0.03	0.01	4.33
SW36	0.59	0.39	0.21	1.18	1.69	0.36	0.73	1.43	0.49	92	0.05	0.02	4.26
SW37	0.53	0.20	0.06	1.06	1.87	0.16	0.77	1.87	0.28	37	0.02	0.01	3.72
SW38	0.23	0.38	0.14	0.46	4.35	0.72	1.24	1.19	0.71	79	0.02	0.10	8.54
SW39	0.68	0.23	0.09	1.36	1.47	0.49	0.68	1.39	0.51	37	0.03	0.01	5.25
SW40	0.56	0.40	0.14	1.12	1.79	1.28	0.75	1.27	0.62	66	0.04	0.05	8.05
SW41	0.76	0.40	0.08	1.52	1.32	0.69	0.65	2.36	0.18	33	0.03	0.02	4.09
SW42	0.68	0.22	0.22	1.36	1.47	0.08	0.68	1.48	0.45	69	0.05	0.01	2.08
SW43	0.55	0.49	0.31	1.10	1.82	0.40	0.76	1.26	0.64	43	0.02	0.01	4.31
SW44	0.57	0.26	0.22	1.14	1.75	0.13	0.75	1.61	0.39	63	0.04	0.00	2.05
SW45	0.33	0.67	0.16	0.66	3.03	0.60	0.98	1.43	0.49	27	0.01	0.05	8.52
SW46	0.82	0.36	0.11	1.64	1.22	0.53	0.62	1.48	0.45	37	0.03	0.02	6.13
SW47	0.64	0.47	0.25	1.28	1.56	0.38	0.70	1.36	0.54	34	0.02	0.01	4.39
SW48	0.22	0.56	0.16	0.44	4.55	0.11	1.19	1.30	0.58	23	0.01	0.06	8.43
SW49	0.44	0.25	0.16	0.88	2.27	0.10	0.85	1.47	0.46	49	0.02	0.01	3.04
SW50	0.61	0.17	0.08	1.22	1.64	0.45	0.72	1.44	0.48	34	0.02	0.01	4.29
SW51	0.62	0.51	0.37	1.24	1.61	0.19	0.71	1.43	0.54	45	0.03	0.01	2.88
SW52	0.36	0.40	0.15	0.72	2.78	0.30	0.94	1.19	0.69	25	0.01	0.03	7.81
SW53	0.75	0.83	0.17	1.50	1.33	1.33	0.65	1.55	0.42	23	0.02	0.03	8.67
SW54	0.50	0.28	0.11	1.00	2.00	1.11	0.79	1.32	0.57	34	0.02	0.02	5.95
SW55	0.64	0.29	0.19	1.28	1.56	0.24	0.70	1.38	0.53	37	0.02	0.01	3.39
SW56	0.39	0.13	0.08	0.78	2.56	0.81	0.89	1.32	0.57	32	0.01	0.01	4.01
SW57	1.19	0.45	0.15	2.38	0.84	0.44	0.52	1.47	0.46	20	0.02	0.01	7.78
SW58	0.93	0.67	0.15	1.86	1.08	0.77	0.58	1.49	0.45	36	0.03	0.03	8.49
SW59	1.00	0.45	0.12	2.00	1.00	0.45	0.56	1.62	0.38	30	0.03	0.01	6.15

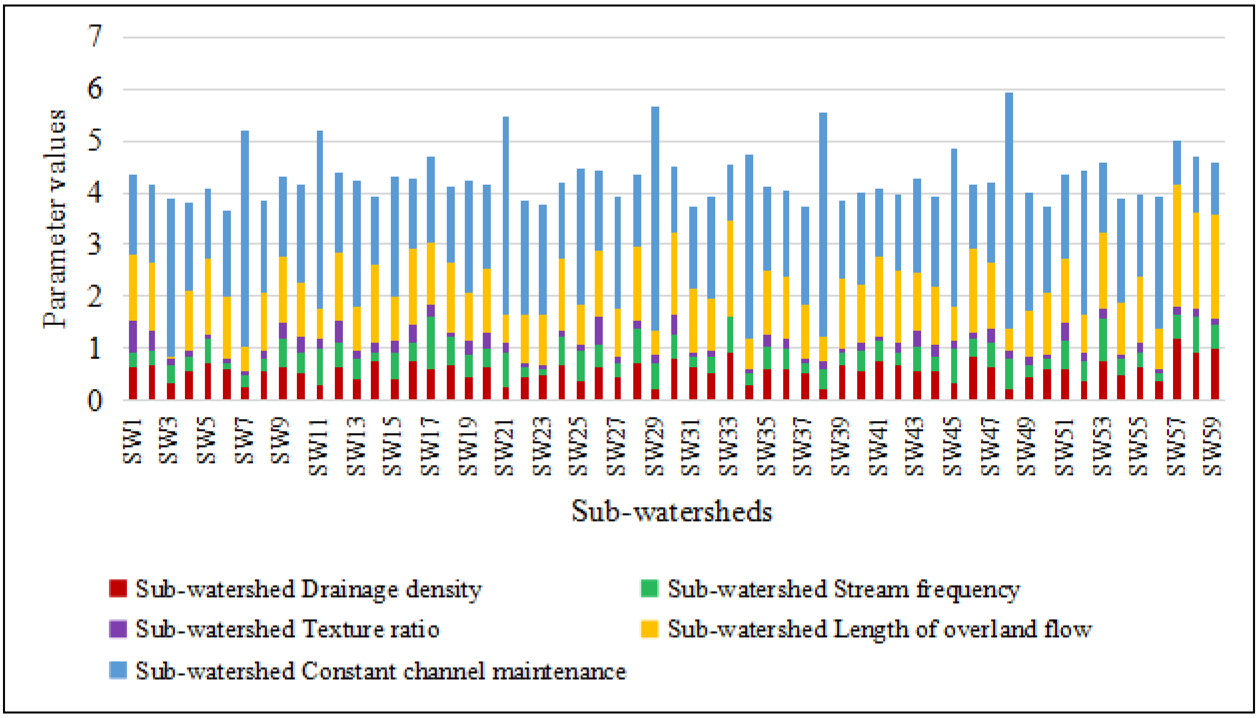

Figure 6: Areal parameter values in the Bunsuru sub-watersheds

Linear characteristics of the Bunsuru watershed

The linear parameters provide insights into the basin's climatic condition, geological structure, rock composition, erosion, and landscape modification history. The linear parameters used to assess sub-watershed susceptibility to erosion include the form factor (Ff), elongation ratio (Re), compactness coefficient (Cc), and circularity ratio (Rc). The form factor (Ff) is a dimensionless ratio that defines the shape of a basin. Sub-watersheds with an elongated form and greater lengths exhibit lower Ff values, while those with more circular shapes tend to show larger Ff values. Basins with wider shapes also show intermediate Ff values (Dali et al., 2023). In the studied watershed, Ff values range from 0.02 in SW 1 to 1.33 in SW 53(Figure 7). Sub-watersheds with lower Ff values are more elongated, indicating lower peak flows over longer durations. In contrast, higher Ff values correspond to sub-watersheds with higher peak flows over shorter durations, as noted by Taib et al. (2023). The elongation ratio (Er) is the ratio of the diameter of a circle with the same area as the basin to the basin's maximum length (Schumm, 1956). The analysis revealed that the Er ranges from 0.36 in SW 18 to 1.24 in SW 38. Lower Er values indicate elongated sub-watersheds, while higher values correspond to circular watersheds. Lower elongation ratios are associated with low-relief areas that are less susceptible to erosion, and vice versa, as observed by Muluneh and Mamo (2017). Similarly, Debelo and Tadele (2017) found a relationship between the elongation ratio and soil erosion in the Diddesa basin, Ethiopia.

The compactness coefficient (Cc) is the ratio of the perimeter of the watershed to the circumference of a circle with an equivalent area. (Horton, 1945). The values of the CC in the Bunsuru watershed are generally more elongated and range from 1.16 in SW 17 to 2.42 in SW 18. Sub-watersheds with high values are more elongated and exhibit high infiltration and low runoff, and thus are less vulnerable to soil erosion (Patel, 2015). The circularity ratio (Rc) is the ratio of the basin's area to the area of a circle with the same circumference as the basin's perimeter, indicating the watershed's dendritic stage. In the study watershed, Rc values range from 0.1 in SW 18 to 0.71 in SW 38. Sub-watersheds with lower Rc values are generally more elongated, while values approaching 1 indicate more circular basins (Strahler, 1964). This variation in Rc can be attributed to differences in relief and slope within the watershed, as similarly observed by Babeesh and Achyuthan (2019) in the Palar River Basin, India.

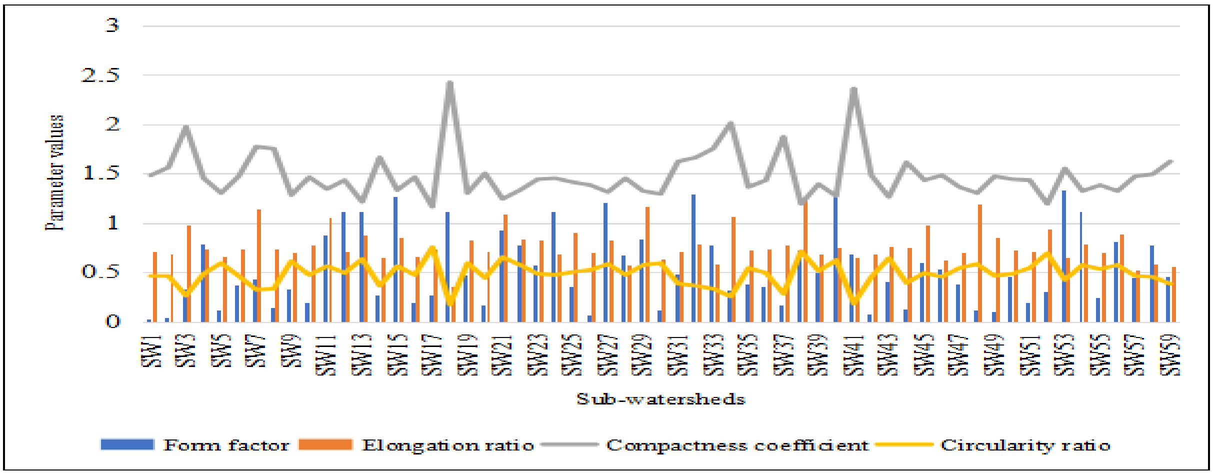

Figure 7: Linear parameters of the Bunsuru sub-watersheds

Relief Characteristics of the Bunsuru Watershed

The watershed relief significantly influences topography and drainage patterns, playing a significant role in identifying soil erosion risk and supporting effective watershed planning and management (Ghosh et al., 2021). It also reflects the changes that have occurred in the landscape over time (Bhunia et al., 2012). Four relief parameters, such as watershed relief (R), ruggedness number (Rn), relief ratio (Rr), and relative relief (R_{vr}), are commonly used for watershed characterization and soil erosion risk identification (Figure 8). Watershed relief refers to the vertical inequality between the highest and lowest elevations. Among the sub-watersheds analyzed, SW 36 exhibits the highest relief, reflecting a significant elevation range. High relief is commonly associated with increased soil erosion potential when combined with other factors such as drainage density, slope gradient, and topographic variation. Therefore, the sub-watershed requires targeted management strategies to mitigate erosion risks and ensure the sustainable conservation of soil resources. This is because steeper slopes associated with high relief encourage surface runoff, thereby increasing erosion and sediment yield (Jourgholami et al., 2021). The ruggedness number (Rn) is calculated as the product of the maximum basin relief (Bh) and drainage density (Dd), with both parameters expressed in consistent units (Adhikari, 2020). It facilitates a better understanding of surface processes, particularly discharge. Within the Bunsuru watershed, the ruggedness number (Rn) ranges from a maximum of 0.05 in SW 2, 26, and 30 to a minimum of 0.01 in SW 3, 7, 11, 21, 25, 29, 34, 45, 48, 52, and 56. Sub-watersheds exhibiting higher Rn values are typically associated with higher discharge, indicating a higher susceptibility to erosion (Jawahar et al., 2019).

The relief ratio (Rr), which is defined as the ratio of total watershed relief to its maximum horizontal length, indicates that SW 2 has the highest Rr value, whereas sub-watersheds 5 and 8 exhibit the lowest. This parameter represents the overall steepness of the basin and is therefore closely associated with its susceptibility to erosion. Consequently, sub-watersheds with higher Rr values are considered more prone to erosion compared to those with lower values, as noted by Duressa. et al. (2024). Relative relief represents the vertical difference between the highest peak and the lowest point within a basin, usually measured along its longest axis parallel to the main river channel. This parameter serves as a valuable indicator for assessing overall basin steepness, topographic variability, and the intensity of erosion processes within the watershed (Kumar & Kshitij, 2017). Sub-watershed 17 has the highest Rvr while SW 1 exhibits the lowest value.

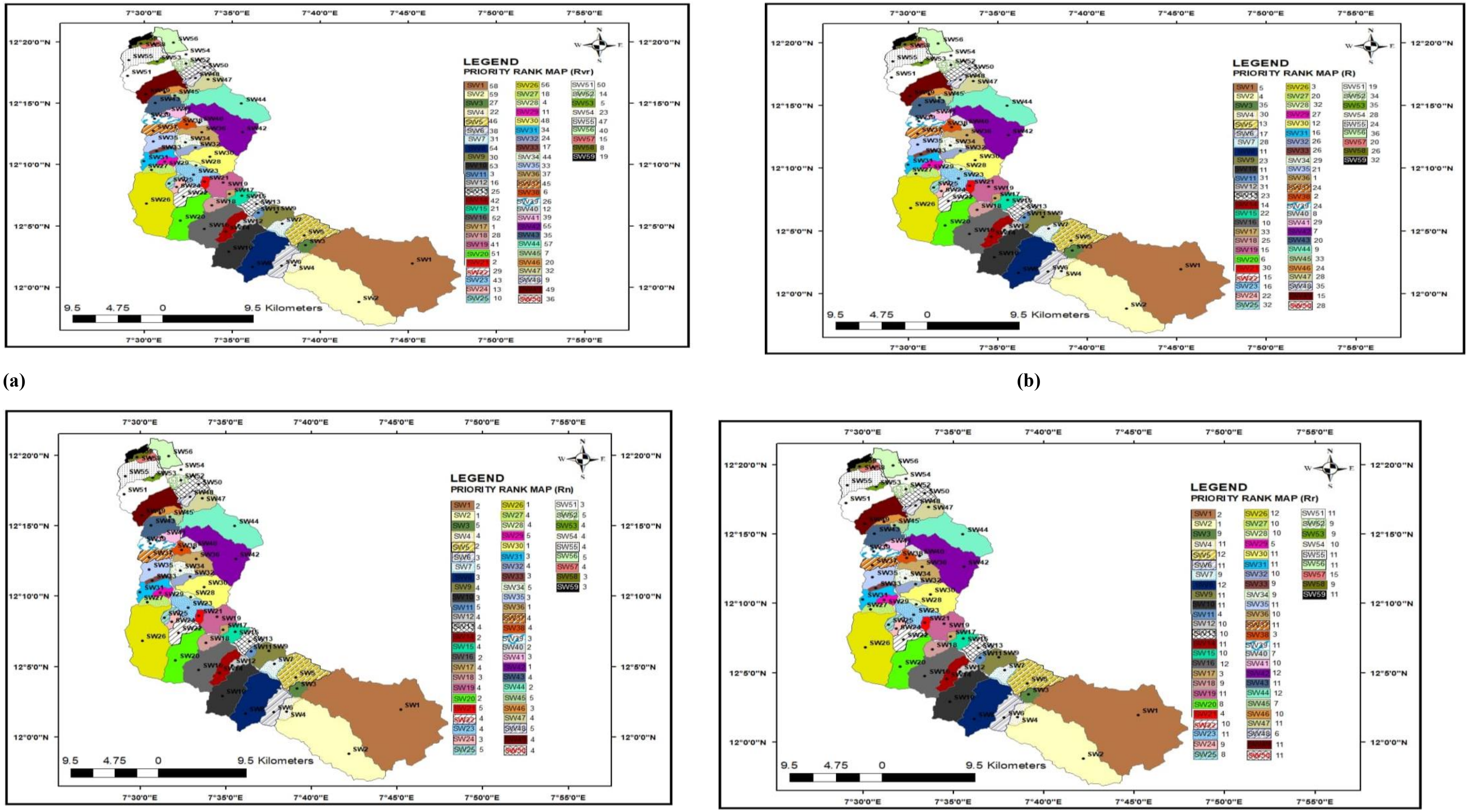

(a) (b)

(c) (d)

Figure 8: Parameters of the Bunsuru sub-watersheds; (a) relative relief, (b) watershed relief, (c) ruggedness number, (d) relief

Prioritization based on morphometric parameters and the weighted sum approach

Watersheds exhibit varying responses to surface runoff based on topographical features, vegetation cover, and other surface characteristics. This variability highlights the need to prioritize critical watersheds to sustain soil and water resources. This study presents the preliminary ranking of sub-watersheds based on morphometric analysis in Table 6. Among the areal parameters, drainage density values indicate that SW 57 ranks first, suggesting a high rate of erosion driven by high hydrological activity and landscape connectivity, similar to the finding of Moeini et al. (2015) in some watersheds within the Ardebil province of Iran. Similarly, stream frequency analysis shows that SW 17 holds the top rank, implying significant erosional activity, as higher runoff volume and velocity are associated with increased erosion potential (Duressa et al., 2024). The results further indicate that SW1 and 43 exhibit the highest texture ratio and length of overland flow, respectively, suggesting a greater susceptibility to erosion, as hydraulic force increases proportionally with flow rate. Additionally, the constant of channel maintenance values shows that SW 48 ranks highest, reflecting the significant influence of drainage density and stream frequency on surface degradation (Singh et al., 2021).

The analysis of linear parameters reveals that SW1 ranks highest in form factor values, indicating the potential for higher peak flows and associated erosion. High flow levels correspond to increased detachment forces due to the kinetic energy of moving water (Chen et al., 2021). Furthermore, elongation ratio values place SW18 at the top, suggesting an elongated watershed characterized by high relief and steep slopes, increasing its susceptibility to erosion (Krishnan, 2024). The compactness coefficient and circularity ratio ranked SW17 and 18 highest, respectively, indicating a tendency for erosion and higher peak flows occurring over shorter durations. The result also revealed that SW36 ranked first in relief and ruggedness number values. Walling (1977) observed a direct relationship between denudation rates and basin relief. In light of these findings, sub-basins characterized by high relief are expected to exhibit high erosion potential.

Table 6: Preliminary Priority Ranking of the Sub-watersheds

Sub-Basin	Areal					Linear					Topographic		
	D_d	F_s	R_t	L_{of}	C_{cm}	F_f	R_e	C_c	R_c	R	R_N	R_r	R_{vr}
SW1	15	21	1	15	34	1	12	23	14	5	2	2	58
SW2	12	24	5	12	37	2	10	27	14	4	1	1	59
SW3	36	18	25	42	8	41	28	34	4	35	5	9	27
SW4	20	25	23	20	27	29	15	20	16	30	4	11	22
SW5	9	11	28	9	40	7	9	9	26	13	2	12	46
SW6	18	35	26	18	30	16	14	22	14	17	3	11	38
SW7	40	27	25	39	4	43	33	32	6	28	5	9	31
SW8	22	28	17	22	25	9	15	31	7	11	3	12	54
SW9	14	7	7	14	35	14	11	7	27	23	4	11	30
SW10	24	18	8	23	21	11	18	21	15	11	3	11	53
SW11	37	3	16	36	7	47	30	13	23	31	5	4	3
SW12	14	12	3	14	35	32	12	18	17	31	4	10	16
SW13	32	18	15	31	12	32	24	3	29	23	4	10	25
SW14	6	33	16	6	43	13	8	30	8	14	2	11	42
SW15	31	9	14	30	13	34	23	12	23	22	4	10	21
SW16	8	17	7	8	41	11	9	21	15	10	2	12	52
SW17	18	1	11	18	29	38	14	1	29	33	4	3	1
SW18	11	7	25	11	38	32	1	37	1	25	3	9	28
SW19	28	15	9	27	16	21	21	9	26	15	4	11	41
SW20	15	17	9	15	33	10	12	25	12	6	2	8	51
SW21	39	5	15	38	5	48	32	4	31	30	5	4	2
SW22	29	30	25	28	15	28	22	12	24	15	4	10	29
SW23	27	34	26	26	18	25	21	19	16	16	4	11	43
SW24	11	7	20	11	38	32	10	20	15	22	3	9	13
SW25	34	6	20	33	10	42	26	17	18	32	5	8	10
SW26	13	14	2	13	36	3	11	15	20	3	1	12	56
SW27	28	25	22	27	16	33	21	10	25	20	4	10	18
SW28	10	5	18	10	39	26	4	20	15	32	4	10	4
SW29	41	10	19	40	3	46	34	11	24	27	5	5	11
SW30	5	11	4	5	44	6	7	29	26	12	1	11	48
SW31	15	31	25	15	33	22	12	29	9	16	3	11	34
SW32	32	20	23	24	20	36	19	30	8	26	4	10	24
SW33	3	5	29	3	46	28	5	31	7	26	3	9	17
SW34	38	25	26	37	6	40	31	35	3	29	5	9	44
SW35	17	14	12	17	31	17	14	13	22	21	3	11	33
SW36	19	16	14	19	28	15	14	18	17	1	1	10	37
SW37	24	30	27	23	22	10	18	33	5	24	4	11	45
SW38	42	17	20	40	2	45	36	2	33	2	4	3	6
SW39	11	28	24	11	38	23	10	16	19	24	3	11	26
SW40	22	15	20	22	24	35	16	6	28	8	2	7	12
SW41	6	15	25	6	43	27	8	36	2	29	3	10	39
SW42	11	29	13	11	38	4	10	23	13	7	1	12	55
SW43	23	9	8	1	23	18	17	5	30	20	4	11	35
SW44	21	25	13	21	26	8	16	28	10	9	2	12	57
SW45	36	5	18	35	8	44	29	18	17	33	5	7	7
SW46	4	19	22	4	45	24	6	23	13	24	3	10	20
SW47	14	11	10	14	35	17	11	14	22	28	4	11	32
SW48	42	6	18	41	1	49	35	9	25	35	5	6	9
SW49	30	26	18	29	14	5	23	22	14	15	4	11	49
SW50	17	32	24	17	31	20	13	20	16	28	4	11	36
SW51	16	8	6	16	32	11	12	18	22	19	3	11	50
SW52	35	15	19	34	9	39	27	2	32	34	5	9	14
SW53	7	2	17	7	42	37	8	26	11	35	4	9	5
SW54	26	23	22	25	19	31	20	11	24	28	4	10	23
SW55	14	22	15	14	35	12	11	15	21	24	4	11	47
SW56	33	35	25	32	11	30	25	11	24	36	5	11	40
SW57	1	13	19	1	48	19	2	22	14	20	4	11	15
SW58	3	4	19	3	46	28	5	24	13	26	3	9	8
SW59	2	13	21	2	47	20	3	29	9	32	3	11	19

FUDMA Journal of Earth and Environmental Sciences (FUDJEES), Vol. 3, No. 1, 2026
Print ISSN: 1595-9686
EISSN: 1595-9708

The correlation matrix indicates several notable relationships among the morphometric parameters (Table 7). A strong positive correlation was observed between drainage density and length of overland flow (r = 0.983), and between the constant of channel maintenance and both the form factor (r = 0.862) and elongation ratio (r = 0.961). In contrast, a strong negative correlation was identified between drainage density and the constant of channel maintenance (r = -0.895), and between drainage density and elongation ratio (r = -0.889). Similarly, the length of overland flow exhibited a negative correlation with the constant of channel maintenance (r = -0.881) and elongation ratio (r = -0.885). Additionally, the constant of channel maintenance showed a strong negative correlation with the circularity ratio (r = -0.946)

Table 7: Correlation Matrix of Morphometric Variables for the Bunsuru Sub-watersheds

Correlation Parameters	D_d	F_s	R_t	L_{of}	C_{cm}	F_f	R_e	C_c	R_c	R	R_N	R_r	R_{vr}
Dd	1.000	0.101	0.116	0.983	-0.895	-0.655	-0.899	0.184	-0.260	0.055	0.572	0.037	-0.150
F_s	0.101	1.000	0.160	0.101	0.031	0.375	-0.038	-0.168	0.264	-0.315	-0.181	-0.077	0.706
R_t	0.116	0.160	1.000	0.133	0.192	-0.168	-0.139	-0.297	0.283	0.454	0.418	0.397	-0.284
L_{of}	0.983	0.101	0.133	1.000	-.0.881	-0.640	-0.885	0.127	-0.202	0.085	0.577	0.039	-0.141
C_{cm}	-0.895	0.031	-0.192	-0.881	1.000	0.862	0.961	-0.147	0.222	-0.172	-0.632	-0.049	0.317
F_f	-0.665	0.375	-0.168	-0.640	0.862	1.000	0.790	-0.175	0.258	-0.307	-0.573	-0.046	0.607
R_e	-0.889	-0.038	-0.139	-0.885	0.961	0.790	1.000	-0.275	0.314	-0.106	-0.600	-0.042	0.269
C_c	0.184	-0.168	-0.297	0.127	-0.147	-0.175	-0.275	1.000	-0.946	-0.122	0.077	0.020	-0.281
R_c	-0.260	0.264	0.283	-0.202	0.222	0.258	0.314	-0.946	1.000	0.093	-0.132	-0.008	0.362
R	0.055	-0.315	0.454	0.085	-0.172	-0.307	-0.106	-0.122	0.093	1.000	0.771	0.310	-0.540
R_N	0.572	-0.181	0.418	0.577	-0.632	-0.573	-0.600	0.077	-0.132	0.771	1.000	0.286	-0.533
Rr	0.037	-0.077	0.397	0.039	-0.049	-0.046	-0.042	0.020	-0.008	0.310	0.286	1.000	-0.209
R_{vr}	-0.150	0.706	-0.284	-0.141	0.317	0.607	0.269	-0.281	0.362	-0.540	-0.533	-0.209	1.000
Sum of Correlation	0.189	1.959	1.881	0.296	0.809	1.328	0.350	-1.003	1.248	1.206	1.050	1.658	1.123
Grand Total	12.094	12.09	12.09	12.09	12.09	12.09	12.09	12.09	12.09	12.09	12.09	12.09	12.09
Weight	0.016	0.162	0.156	0.024	0.066	0.109	0.029	-0.083	0.103	0.099	0.087	0.137	0.093

The prioritization of sub-watersheds based on compound factor values is presented in Table 8. The analysis indicates that these values range from 12.787 in SW1 to 26.372 in SW56 (Figure 9). Notably, sub-watersheds SW23, SW25, SW38, SW50, and SW56 exhibit the highest compound factor values, recorded at 22.651, 22.388, 24.383, 22.174, and 26.372, respectively. In contrast, SW1, SW3, and SW30 display the lowest values, measured at 12.787, 13.407, and 13.884, respectively. This variation in compound factor values reflects the spatial heterogeneity of morphometric characteristics across the sub-watersheds. Sub-watersheds with higher compound factor values are generally associated with lower susceptibility to erosion, increased geomorphic stability, and reduced sediment yield. Conversely, sub-watersheds with lower compound factor values are more prone to erosion, indicating potential instability and higher sediment production (Al-Saady et al., 2016).

Table 8: Priority Ranking of the Sub-Watershed Based on Compound Factor Value

Sub-Basin	Compound Factor Value	Prioritized Rank
SW1	12.787	1
SW2	13.407	2
SW3	16.323	20
SW4	20.647	46
SW5	19.488	43
SW6	21.156	49
SW7	21.039	48
SW8	17.298	27
SW9	16.063	18
SW10	15.795	16
SW11	16.516	22
SW12	15.617	13
SW13	20.546	45
SW14	17.876	33
SW15	17.311	28
SW16	15.778	15
SW17	16.083	19
SW18	15.104	9
SW19	18.018	36
SW20	14.751	7
SW21	17.888	34
SW22	21.952	54
SW23	22.651	57
SW24	15.746	14
SW25	22.388	56
SW26	13.993	4
SW27	20.957	47
SW28	14.685	6
SW29	18.773	38
SW30	13.884	3
SW31	18.829	39
SW32	18.569	37
SW33	15.484	11
SW34	21.292	51
SW35	17.228	26
SW36	19.081	40
SW37	19.264	42
SW38	24.383	58
SW39	21.216	50
SW40	17.720	31
SW41	17.930	35
SW42	17.369	29
SW43	16.505	21
SW44	16.692	23
SW45	16.768	24
SW46	17.612	30
SW47	17.089	25
SW48	19.245	41
SW49	17.845	32
SW50	22.174	55
SW51	15.602	12
SW52	21.864	53
SW53	14.779	8
SW54	21.575	52
SW55	19.921	44
SW56	26.372	59
SW57	15.253	10
SW58	14.124	5
SW59	16.054	17

The final ranking of the sub-watersheds, based on compound factor values and weighted sum analysis, is presented in Table 9. Sub-watersheds 1, 2, and 30 fall under the very high vulnerability class, collectively accounting for 31.8% of the total area. Additionally, sub-watersheds 9, 10, 11, 12, 16, 17, 18, 20, 24, 26, 28, 33, 43, 44, 45, 51, 53, 57, 58, and 59 are categorized as having high erosion risk, representing 28.1% of the basin area (Figure 10). Sub-watersheds classified within the very high and high susceptibility categories suggest areas experiencing intense soil erosion, which may contribute significantly to increased sediment deposition in the downstream reservoir. These findings are consistent with the work of Godif and Manjunatha (2022), who reported that 36% of the Geba Basin in Tigray, Ethiopia, exhibited high erosion susceptibility. The pronounced vulnerability in these sub-watersheds is attributed to their high ruggedness number and relatively high relief, suggesting higher discharge and greater susceptibility to erosion. These insights underscore critical areas for targeted soil and water conservation interventions, which are vital for sustainable river basin management and planning (Raja Shekar & Mathew, 2024).

Sub-watersheds 3, 5, 8, 14, 15, 19, 21, 29, 31, 32, 35, 36, 37, 40, 41, 42, 46, 47, 48, 49, and 55 are classified as having moderate erosion vulnerability, collectively accounting for 27.6% of the basin area. Sub-watersheds 4, 6, 7, 13, 22, 27, 34, 39, 52, and 54 are categorized as low erosion risk zones, covering 8% of the total basin area. Meanwhile, sub-watersheds 23, 25, 38, 50, and 56 fall into the very low erosion risk category, comprising 4.5% of the study area. These sub-watersheds, characterized by moderate to very low erosion susceptibility, are associated with relatively minimal soil erosion and consequently lower sediment yield. This condition is likely due to the relatively low relief in these regions, where gentle slopes promote increased infiltration, reduced surface runoff, and, ultimately, lower erosion potential.

FUDMA Journal of Earth and Environmental Sciences (FUDJEES), Vol. 3, No. 1, 2026
Print ISSN: 1595-9686
EISSN: 1595-9708

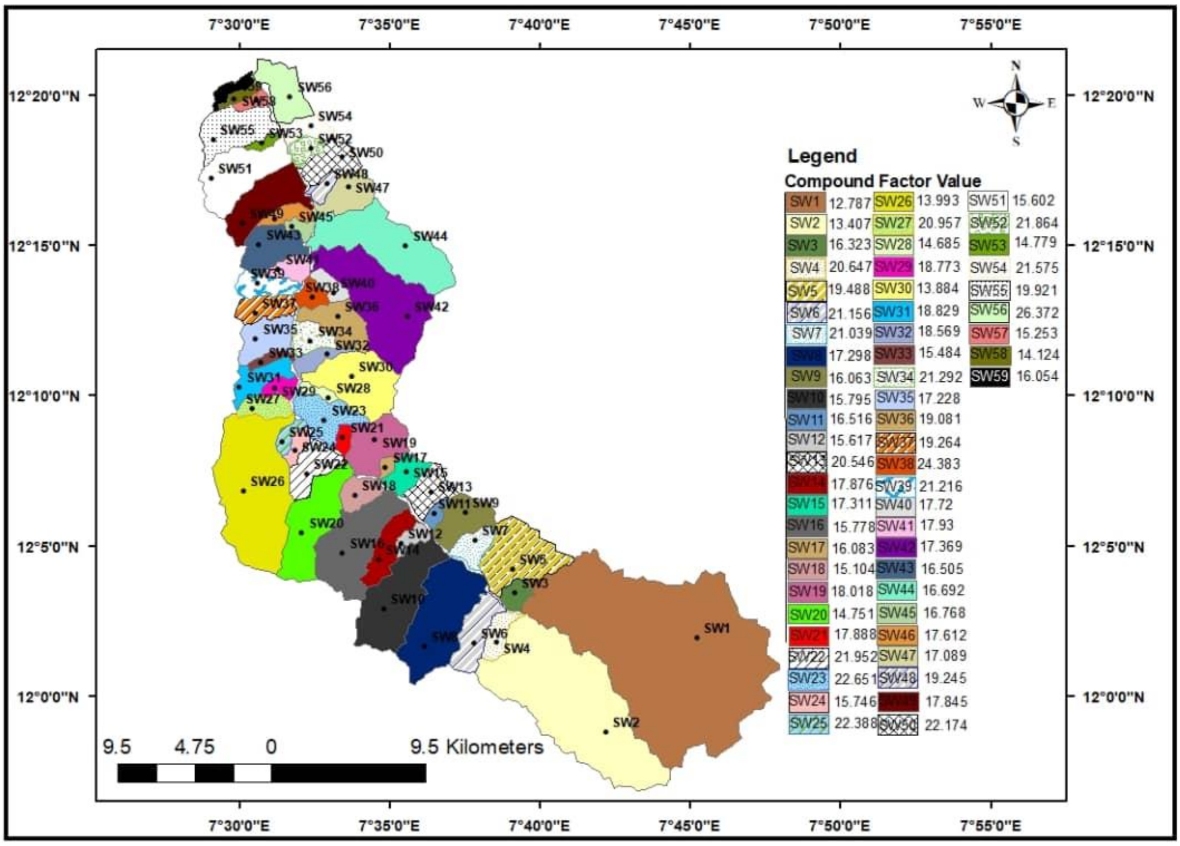

Figure 9: Compound factor values and rank of sub-watersheds

Table 9: Soil Erosion Susceptibility Status and Corresponding Areal Coverage

Serial No.	Priority Class	Priority Level	Sub-watershed	Area Coverage (%)
1	12.787 -13.931	Very High	1, 2, 30	31.8
2	13.932-16.953	High	9,10, 11, 12, 16, 44, 45, 17, 18, 20, 24, 26, 28, 33, 43, 51, 53, 57, 58, 59	28.1
3	16.954-19.974	Moderate	3, 5, 14, 15, 8, 19, 21, 29, 31, 32, 35, 36, 37, 40, 41, 42, 46, 47, 48, 49, 55	27.6
4	19.975-21.996	Low	4, 6, 7, 13, 22, 27, 34, 39, 52, 54	8.0
5	>21.95	Very Low	23, 25, 38, 50, 56	4.5

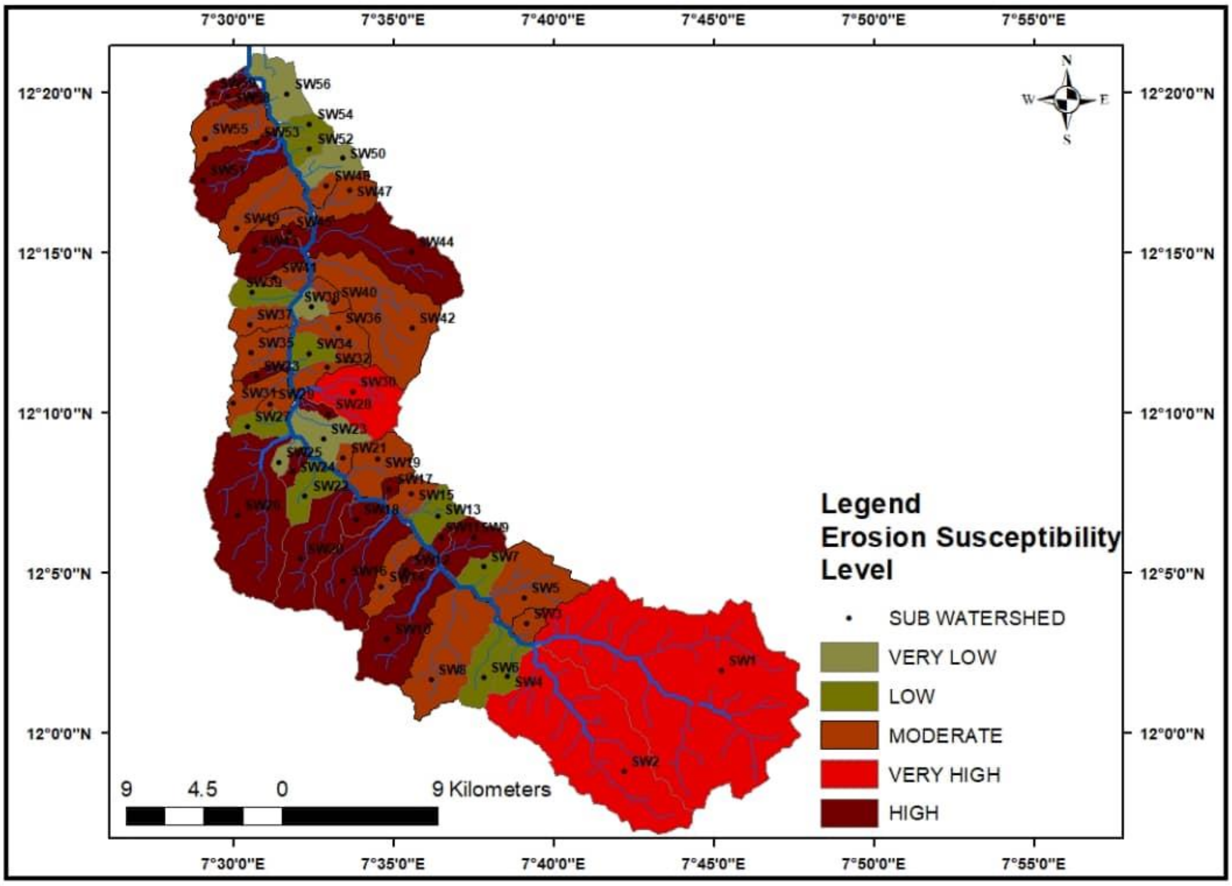

Figure 10: Erosion priority class of the sub-watersheds.

SUMMARY AND CONCLUSION

This study aimed to characterize and prioritize the Bunsuru watershed into erosion hazard zones to facilitate the targeted implementation of soil and water conservation strategies. As one of the largest watersheds in Katsina State and the primary contributing catchment to the Zobe Reservoir, the State's largest irrigation facility, the Bunsuru watershed is critical for regional water resource management. However, it remains susceptible to soil erosion, sedimentation, and declining water quality. To achieve this aim, the study employed an integrated approach that combined SRTM-DEM data, Geographic Information Systems (GIS), and a statistical correlation-based weighted sum method. The watershed was categorized into 59 sub-watersheds. Morphometric parameters sensitive to erosion were considered as input in prioritizing the sub-watersheds. These variables were used to generate the compound factor values and the weight of each parameter in each sub-watershed.

The results indicate that sub-watersheds 1, 2, and 30 fall into the very high vulnerability class, accounting for 31.8% of the total area. Additionally, sub-watersheds 9, 10, 11, 12, 16, 17, 18, 20, 24, 26, 28, 33, 43, 44, 45, 51, 53, 57, 58, and 59 are categorized as having high erosion risk, representing 28.1%. However, sub-watersheds 3, 5, 8, 14, 15, 19, 21, 29, 31, 32, 35, 36, 37, 40, 41, 42, 46, 47, 48, 49, and 55 fall within the moderate erosion risk zones and account for 27.6% of the area. Furthermore, sub-watersheds 4, 6, 7, 13, 22, 27, 34, 39, 52, and 54 are classified as low erosion risk zones, covering 8% of the area. Meanwhile, sub-watersheds 23, 25, 38, 50, and 56 fall into the very low erosion risk category, occupying 4.5% of the area.

The findings of this study underscore the urgent need for targeted intervention in sub-watersheds identified as having a high erosion risk. To promote the sustainable management of soil and water resources, it is recommended that conservation strategies such as afforestation, enforcement of forest protection policies, and regulation of land use practices be implemented. These measures are expected to enhance water infiltration, reduce surface runoff, and minimize soil erosion in ungauged watersheds such as that of Bunsuru, where data on soil erosion remain limited. Furthermore, the watershed's expansive and inaccessible nature presents challenges to field-based observation, highlighting the need for adequate resources, time, and skilled personnel. Therefore, the outcomes of this research offer a viable alternative for guiding the strategic application of land resource conservation efforts in this data-scarce environment.

CONFLICT OF INTEREST DISCLOSURE STATEMENT

The authors reported no potential conflict of interest.

REFERENCES

Abdeta, G. C., Bekele, A., Abiyot, T., Tura, L., & Haile, G. (2020). Morphometric analysis for prioritizing sub-watersheds and management planning and practices in Gidabo Basin, Southern Rift Valley of Ethiopia. *Applied Water Science*, *10*(158). https://doi.org/10.1007/s13201-020-01239-7

Adesoji, I., Byami, J., & Mam, T. (2024). Assessment of Chemical Characteristics of Bottom Sediments of Zobe Dam Reservoir, Katsina State, Nigeria. *Dutse Journal of Pure and Applied Sciences*, *10*(1), 110–117.

Adhikari, S. (2020). Morphometric Analysis of a Drainage Basin: A Study of. *The Geographic Base*, *7*, 127–144. https://doi.org/10.3126/tgb.v7i0.34280

Aher, P. D., Adinarayana, J., & Gorantiwar, S. D. (2014). Quantification of morphometric characterization and prioritization for management planning in semi-arid tropics of India: A remote sensing and GIS approach. *Journal of Hydrology*, *511*, 850–860. https://doi.org/10.1016/j.jhydrol.2014.02.028

Al-Saady, Y. I., Al-Suhail, Q. A., Al-Tawash, B. S., & Othman, A. A. (2016). Drainage network extraction and morphometric analysis using remote sensing and GIS mapping techniques (Lesser Zab River Basin, Iraq and Iran). *Environmental Earth Sciences*, *75*, 1–23.

Altaf, F., Meraj, G., & Romshoo, S. A. (2013). Morphometric Analysis to Infer Hydrological Behaviour of Lidder Watershed, Western Himalaya, India. *Geography Journal*, *2013*. https://doi.org/10.1155/2013/178021

Arrington, W. (2021). Soil Erosion, Causes and Effects. *International Journal of Agriculture, Environment and Bioresearch*, *06*(06), 226–235.

Babeesh, C., & Achyuthan, H. (2019). Quantitative analysis of the drainage and morphometric characteristics of the Palar River basin, Southern Peninsular India; using bAd calculator (bearing azimuth and drainage) and GIS. *Geology, Ecology, and Landscapes*, *3*(4), 295–307. https://doi.org/10.1080/24749508.2018.1563750

Bagarello, V., Ferro, V., & Scienze, V. (2010). Analysis of soil loss data from plots of differing length for the Sparacia experimental area, Sicily, Italy. *Biosystems Engineering*, *105*(3), 411–422. https://doi.org/10.1016/j.biosystemseng.2009.12.015

Benzougagh, B., Meshram, S. G., Dridri, A., Boudad, L., Baamar, B., Sadkaoui, D., & Khedher,

K. M. (2022). Identification of critical watershed at risk of soil erosion using morphometric and geographic information system analysis. *Applied Water Science*, *12*(1), 1–20. https://doi.org/10.1007/s13201-021-01532-z

Bhunia, G. S., Samanta, S., & Pal, B. (2012). Quantitative analysis of relief characteristics using space technology. *International Journal of Physical and Social Sciences*, *2*(8), 350–365.

Callow, J. N., Niel, K. P. Van, & Boggs, G. S. (2007). How does modifying a DEM to reflect known hydrology affect subsequent terrain analysis? *Journal of Hydrology*, *332*, 30–39. https://doi.org/10.1016/j.jhydrol.2006.06.020

Chen, C., Lei, T., & Ban, Y. (2021). Influence of slope, flow rate, and thawed depth on soil detachment rate in partially thawed black soils—Journal *of Hydrology*, *603*, 127009.

Choudhari, P. P., Nigam, G. K., Singh, S. K., & Thakur, S. (2018a). Morphometric-based prioritization of watershed for groundwater potential of Mula river basin, Maharashtra, India. *Geology, Ecology, and Landscapes*, *2*(4), 256–267. https://doi.org/10.1080/24749508.2018.1452482

Choudhari, P. P., Nigam, G. K., Singh, S. K., & Thakur, S. (2018b). Morphometric-based prioritization of watershed for groundwater potential of Mula river basin, Maharashtra, India. *Geology, Ecology, and Landscapes*, *9508*, 1–12. https://doi.org/10.1080/24749508.2018.1452482

Dali, N., Ziouch, O. R., Dali, H., Daifallah, T., Cherifa, B., & Sara, H. (2023). Remote sensing and GIS approach for morphometric assessment and sub-watershed prioritization according to soil erosion and groundwater potential in an endorheic semi-arid area of Algeria—Arabian *Journal of Geosciences*, *16*(1), 95.

Dar, I. A., Prabu, P., & Dar, M. A. (2013). Erosion Modeling in Hard Rock Terrain Using Morphometry: A Case Study from Tamil Nadu, India. *Environmental Quality Management*, *23*(2), 47–60. https://doi.org/10.1002/tqem.21360

Debelo, G., & Tadele, K. (2017). Morphometric Analysis to Identify Erosion Prone Areas in the Upper Blue Nile (Case study of the Diddesa and Jamena Basins, Ethiopia). *International Research Journal of Engineering and Technology*, *4*(8), 1773–1784.

Dofee, A. A., Chand, P., & Kumar, R. (2024). Prioritization of soil erosion-prone sub-watersheds using geomorphometric and statistical-based weighted sum priority approach in the middle Omo-Gibe River basin, Southern Ethiopia. *International Journal of Digital Earth*, *17*(1), 1–32. https://doi.org/10.1080/17538947.2024.2350198

Dragičević, N., Karleuša, B., & Ožanić, N. (2019). Different approaches to estimation of drainage density and their effect on the Erosion Potential Method. *Water (Switzerland)*, *11*(3), 1–14. https://doi.org/10.3390/w11030593

Duressa, A. A., Feyissa, T. A., Tukura, N. G., & Gudeta, Beekan Gurmessa, Gadefa Fekadu Gechelu, T. S. B. (2024). Identification of soil erosion-prone areas for effective mitigation measures using a combined approach of morphometric analysis and geographical information system. *Results in Engineering*, *21*(November 2023), 101712. https://doi.org/10.1016/j.rineng.2023.101712

Duressa, A. A., Feyissa, T. A., Tukura, N. G., Gudeta, B. G., Fekadu Gechelu, G., & Bibi, T. S.

(2024). Identification of soil erosion-prone areas for effective mitigation measures using a combined approach of morphometric analysis and geographical information system. *Results in Engineering*, *21*(December 2023), 101712. https://doi.org/10.1016/j.rineng.2023.101712

El Brahimi, M., Mastere, M., Benzougagh, B., El Fellah, B., Fartas, N., Ladel, L., Sbihi, A., Turyasingura, B., Alsulamy, S., Khedher, K. M., Shohan, A. A. A., Salem, M. A., & Alluqmani, A. E. (2024). Assessing soil erosion vulnerability through geospatial morphometric analysis in the Oued Amter Basin (Northwest Morocco). *Euro-Mediterranean Journal for Environmental Integration*, *May*. https://doi.org/10.1007/s41207-024-00493-4

Farhan, Y., Anbar, A., Al-Shaikh, N., & Mousa, R. (2017). Prioritization of Semi-Arid Agricultural Watershed Using Morphometric and Principal Component Analysis, Remote Sensing, and GIS Techniques, the Zerqa River Watershed, Northern Jordan. *Agricultural Sciences*, *08*(01), 113–148. https://doi.org/10.4236/as.2017.81009

Forkuor, G., & Maathuis, B. (2012). Comparison of SRTM and ASTER Derived Digital Elevation Models over Two Regions in Ghana - Implications for Hydrological and Environmental Modeling. In *Studies on Environmental and Applied Geomorphology* (Issue March 2012). https://doi.org/10.5772/28951

Gajbhiye, S., Mishra, S. K., & Pandey, A. (2014). Prioritizing erosion-prone area through morphometric analysis: an RS and GIS perspective. *Applied Water Science*, *4*(1), 51–61. https://doi.org/10.1007/s13201-013-0129-7

Ghosh, P. K., Mukhopadhyay, R., & Jana, N. C. (2021). Quantitative Analysis of Drainage Basin Parameters towards better Management of Damodar River, Eastern India. *Journal of the Geological Society of India*, *97*(7), 711–734. https://doi.org/10.1007/s12594-021-1753-8

Godif, G., & Manjunatha, B. R. (2022). Heliyon Prioritizing sub-watersheds for soil and water conservation via morphometric analysis and the weighted sum approach: A case study of the Geba river basin in Tigray, Ethiopia. *Heliyon*, *8*(December), e12261. https://doi.org/10.1016/j.heliyon.2022.e12261

Hassan, M. & Kabir, A. (2019). Morphometric and Vulnerability Analysis of Gada River Basin to Erosion and Sediment Yield. *Fudma Journal of Sciences*, *38*(3), 3–6.

Hegazy, I. R., & Kaloop, M. R. (2015). Monitoring urban growth and land use change detection with GIS and remote sensing techniques in Daqahlia governorate, Egypt. *International Journal of Sustainable Built Environment*, *4*(1), 117–124. https://doi.org/10.1016/j.ijsbe.2015.02.005

Horton, R. E. (1945a). Erosional development of streams and their drainage basins, hydrologic approach to quantitative morphology. *Geological Society of America Bulletin*, *56*(3), 275–370. https://doi.org/10.1130/0016-7606(1945)56

Horton, R. E. (1945b). Erosional development of streams and their drainage basins; hydrophysical approach to quantitative morphology. *Geological Society of America Bulletin*, *56*(3), 275–370.

Jawahar, R. S. N., Sivasankar, R. V, & Omine, P. A. K. (2019). Geo - spatial technique - based approach on drainage morphometric analysis at Kalrayan Hills, Tamil Nadu, India.

Applied Water Science, *9*(1), 1–18. https://doi.org/10.1007/s13201-019-0899-7

Jourgholami, M., Karami, S., Tavankar, F., Lo Monaco, A., & Picchio, R. (2021). Effects of slope gradient on runoff and sediment yield on machine-induced compacted soil in temperate forests. *Forests*, *12*(1), 1–19. https://doi.org/10.3390/f12010049

Kadam, A. K., Jaweed, T. H., Kale, S. S., Umrikar, B. N., & Sankhua, R. N. (2019). Identification of erosion-prone areas using modified morphometric prioritization method and sediment production rate: a remote sensing and GIS approach. *Geomatics, Natural Hazards and Risk*, *10*(1), 986–1006. https://doi.org/10.1080/19475705.2018.1555189

Kandpal, H., Kumar, A., Reddy, C. P., & Malik, A. (2017). Watershed prioritization based on morphometric parameters using remote sensing and geographical information system. *Indian Journal of Ecology*, *44*(3), 433–437.

Krishnan, A. (2024). Morphometric analysis in the sub-basins of the Kali River using Geographic Information System, Karnataka, India. *Geomatica*, *76*(2), 100013.

Kumar, A. (2021). Watershed prioritization for soil erosion mapping for the Lesser Himalayan Indian basin using PCA, WSA method in conjunction with morphometric parameters and GIS-based approach. *Research Square*.

Kumar, P., & Kshitij, R. (2017). A GIS-based approach in drainage morphometric analysis of Kanhar River Basin, India. *Applied Water Science*, 217–232. https://doi.org/10.1007/s13201-014-0238-y

Maderal, E. N., Valcarcel, N., Delgado, J., Sevilla, C., & Ojeda, J. C. (2016). Automatic River Network Extraction from LIDAR Data. *The International Archives of the Photogrammetry, Remote Sensing and Spatial Information Sciences, Volume XLI-B8, 2016 XXIII ISPRS Congress, 12–19 July 2016, Prague, Czech Republic*, *XLI*(July), 12–19. https://doi.org/10.5194/isprsarchives-XLI-B8-365-2016

Malik, A., Kumar, A., & Kandpal, H. (2019). *Morphometric analysis and prioritization of sub-watersheds in a hilly watershed using weighted sum approach*.

Marcellus, A., & Ehiomogue, P. (2017). *A Review of the Causes, Effects and Way out of Soil Erosion on Agricultural Lands*. *9*(4), 1–11.

Moeini, A., Zarandi, N. K., Pazira, E., & Badiollahi, Y. (2015). The relationship between drainage density and soil erosion rate: a study of five watersheds in Ardebil Province, Iran. *River Basin Management VIII*, *1*, 129–138. https://doi.org/10.2495/rm150121

Muluneh, T., & Mamo, W. (2017). *Morphometric Analysis of Didessa River Catchment in Blue Nile Basin, Original Research Morphometric Analysis of Didessa River Catchment in Blue Nile Basin*, *July*. https://doi.org/10.4314/star.v3i3.31

Nwilo, P. C., Ogbeta, C. O., Daramola, O. E., Okolie, C. J., & Orji, M. J. (2021). Soil Erosion Susceptibility Mapping of Imo River Basin Using Modified Geomorphometric Prioritisation Method. *Quaestiones Geographicae*, *40*(3), 143–162. https://doi.org/10.2478/quageo-2021-0029

Obeidat, M., Awawdeh, M., & Al-Hantouli, F. (2021). Morphometric analysis and prioritisation of watersheds for flood risk management in Wadi Easal Basin (WEB), Jordan, using geospatial technologies. *Journal of Flood Risk Management*, *14*(2), 1–19.

https://doi.org/10.1111/jfr3.12711

Obialor, C. A., Okeke, O. C., Onunkwo, A. A., Fagorite, V. I., & Ehujuo, N. N. (2019). Reservoir Sedimentation: Causes, Effects, and Mitigation. *International Journal of Advanced Academic Research*, *5*(10), 92–109.

Odiji, C. A., Aderoju, O. M., Eta, J. B., Shehu, I., Mai-Bukar, A., & Onuoha, H. (2021). Morphometric analysis and prioritization of upper Benue River watershed, Northern Nigeria. *Applied Water Science*, *11*(2), 1–28. https://doi.org/10.1007/s13201-021-01364-x

Oruonye, E. D., & Ahmed, Y. M. (2021). Evaluation of Erosion-Prone Areas in Lamurde River Basin, Nigeria Using Morphometric Prioritization Method. *Journal of Geography, Environment and Earth Science International*, *25*(8), 17–31. https://doi.org/10.9734/jgeesi/2021/v25i830301

Patel, D. P. (2015). Prioritization of Malesari mini-watersheds through morphometric analysis: A remote sensing and GIS perspective Prioritization of Malesari mini-watersheds through morphometric analysis: a remote sensing and GIS perspective. *Environmental Earth Sciences*, *August 2012*. https://doi.org/10.1007/s12665-012-2086-0

Raja Shekar, P., & Mathew, A. (2024). Morphometric analysis of watersheds: A comprehensive review of data sources, quality, and geospatial techniques. *Watershed Ecology and the Environment*, *6*(November 2023), 13–25. https://doi.org/10.1016/j.wsee.2023.12.001

Reuben A. Heine, Christopher L. Lant, & R. R. S. (2004). Development and Comparison of Approaches for Automated Mapping of Stream Channel Networks. *Annals of the Association of American Geographers, 94(3), 2004, Pp. 477–490*, *94*(September 2002), 477–490.

Schumm, S. A. (1956). Evolution of drainage systems and slopes in badlands at Perth Amboy, New Jersey. *Geological Society of America Bulletin*, *67*(5), 597–646.

Sharma, S. K., Gajbhiye, S., & Tignath, S. (2015). Application of principal component analysis in grouping geomorphic parameters of a watershed for hydrological modeling. *Applied Water Science*, *5*(1), 89–96. https://doi.org/10.1007/s13201-014-0170-1

Shekar, P. R., Mathew, A., Arun, P. S., & Gopi, V. P. (2023). Sub-watershed prioritization using morphometric analysis, principal component analysis, hypsometric analysis, land use/land cover analysis, and machine learning approaches in the Peddavagu River Basin, India. *Journal of Water and Climate Change*, *14*(7), 2055–2084. https://doi.org/10.2166/wcc.2023.221

Shortridge, A. (2013). Shuttle Radar Topography Mission Elevation Data Error and Its Relationship to Land Cover. *Cartography and Geographic Information Science*, *33*(1), 37–41. https://doi.org/10.1559/152304006777323172

Singh, W. R., Barman, S., & Tirkey, G. (2021). Morphometric analysis and watershed prioritization in relation to soil erosion in Dudhnai Watershed. *Applied Water Science*, *11*(9), 1–12. https://doi.org/10.1007/s13201-021-01483-5

Strahler, A. N. (1956). Quantitative Slope Analysis. *Bulletin of the Geological Society of America*, *67*(20), 571–596.

Strahler, A. N. (1957). Quantitative analysis of watershed geomorphology. *Eos, Transactions American Geophysical Union*, *38*(6), 913–920.

Strahler, A. N. (1964). Part II. Quantitative geomorphology of drainage basins and channel networks. *Handbook of Applied Hydrology: McGraw-Hill, New York*, 4–39.

Taib, H., Hadji, R., & Hamed, Y. (2023). Erosion patterns, drainage dynamics, and their environmental implications: a case study of the Hammamet basin using advanced geospatial and morphometric analysis. *Journal of Umm Al-Qura University for Applied Sciences*, *0123456789*. https://doi.org/10.1007/s43994-023-00096-9

Thakkar, A. K., & Dhiman, S. D. (2007). Morphometric analysis and prioritization of miniwatersheds in Mohr watershed, Gujarat using remote sensing and GIS techniques. *Journal of the Indian Society of Remote Sensing*, *35*, 313–321.

Turcotte, R., Fortin, J., Rousseau, A. N., Massicotte, S., & Villeneuve, J. (2001). *Determination of the drainage structure of a watershed using a digital elevation model and a digital river and lake network*. *240*, 225–242.

Wagh, S. M., V. (2023). A GIS-based Morphometric Prioritization of Watersheds for Soil Erosion Planning: A Case Study. *Research Square*. https://doi.org/DOI: https://doi.org/10.21203/rs.3.rs-1913741/v1

Wagh, S. (2022). *A GIS-based Morphometric Prioritization of Watersheds for Soil Erosion Planning: A Case Study*.

Walling, D. (1977). Assessing the Accuracy of Suspended Sediment Rating Curve for Small Basin. *Water Resource Research*, *13*(3), 531–538.

Yang, L. (2011). SRTM DEM and its application advances. *International Journal of Remote Sensing*, *32*(14), 3875–3896. https://doi.org/10.1080/01431161003786016

Yonnana E., Dzarma, M.S., David, N., Soyi, D.F, Ja'afaru, W. (2020). Morphometric Analysis and Prioritization of Muvur Sub-Basins for Soil Erosion Vulnerability in the Muvur Watershed, Mubi, Northeastern Nigeria. *The Environmental Studies Journal*, *3*(2), 64–76